Numerical methods for a four dimensional hyperchaotic system with applications

by

Abram Hlophane Sibiya

submitted in accordance with the requirements
for the degree of

MASTER OF SCIENCE

in the subject

APPLIED MATHEMATICS

in the

Department of Mathematical Sciences

at the

University of South Africa

Supervisor: Prof. Emile Franc Doungmo Goufo

(December 2019)

Preface

This study was carried out at the University of South Africa in the Mathematical Sciences Department, the science campus Florida in South Africa, from the year 2018 to the year 2019, under the supervision of Professor Emile Franc DOUNGMO GOUFO. The study in this dissertation is the original work of the researcher and has not been submitted in any form for any degree or diploma at any tertiary institution. Where use has been made of works by other authors, they have been duly acknowledged.

Abstract

This study seeks to develop a method that generalises the use of Adams-Bashforth to solve or treat partial differential equations with local and non-local differentiation by deriving a two-step Adams-Bashforth numerical scheme in Laplace space. The resulting solution is then transformed back into the real space by using the inverse Laplace transform. This is a powerful numerical algorithm for fractional order derivative. The error analysis for the method is studied and presented. The numerical simulations of the method as applied to the four-dimensional model, Caputo-Lu-Chen model and the wave equation are presented.

In the analysis, the bifurcation dynamics are discussed and the periodic doubling processes that eventually caused chaotic behaviour (butterfly attractor) are shown. The related graphical simulations that show the existence of fractal structure that is characterised by chaos and usually called strange attractors are provided.
For the Caputo-Lu-Chen model, graphical simulations have been realised in both integer and fractional derivative orders.

Key terms: Chaotic system, Hyperchaotic system, Ordinary Differential Equation, Initial Value Problem, Laplace Transform, Adams-Bashforth, Fractional Calculus, Atangana-Baleanu, Partial Differential Equation, Fractional Differential Equation

List of Acronyms

O.D.E	:	Ordinary Differential Equation
P.D.E	:	Partial Differential Equation
IVP	:	Initial Value Problem
FDE	:	Fractional Differential Equation
CFFD	:	New Caputo-Fabrizio derivative with fractional order
ABC	:	Atangana-Baleanu in the Caputo sense
2-GRL	:	Goufo-Riemann-Liouville

Declaration - Plagiarism

Name: Abram Hlophane Sibiya

Student number: 3085-691-4

Degree: Master of Science: Applied Mathematics

Numerical methods for a four dimensional hyperchaotic system with applications

I hereby declare that the above dissertation is my own work and has not been copied from another person. All the sources that I have used were properly cited. In the event that I used ideas or words, I have paraphrased them and clearly stated the sources from which they come from.

Further,I would like to declare that this work or any part of it, was never previously submitted for examination purpose at the university of South Africa or another institution of higher education.

SIGNED BY

(Abram H. Sibiya)

17/02/2020

DATE SIGNED

Dedication

This dissertation is dedicated to my parents who throughout the years of my studies have consistently encouraged and fully supported me.

Acknowledgements

I give thanks to God, the Almighty, for HIS guiding light that led me through the journey.

My sincere gratitude and lots of thanks go to my supervisor Professor Emile Franc DOUNGMO GOUFO for his assistance among other things in formulating the research topic as well as the research methodology. His dedication, time and guidance are very much appreciated.

I would like to thank and express my appreciation to my family and friends for their unwavering support and encouragement throughout my studies and in particular during the writing of this work. Many thanks to my fiancé who afforded me time and space to work throughout this dissertation.

Finally, I am extremely grateful for this opportunity given to me by the University of South Africa (UNISA) to do this study. It is very much appreciated.

Contents

List of Figures

Chapter 1

Introduction

It is well known that chaos theory was developed from the observation of weather patterns. Since then, chaos theory has become applicable to a number of various occurrences in real life. Domains like robotics, computer science, geology, mathematics, microbiology, biology, population dynamics, economics, philosophy, anthropology, physics, politics and psychology evolved through the use of chaos theory. Mathematically, life phenomena are expressed in terms of differential equations or systems of differential equations. Some systems are simply chaotic characterised by its [36] extreme sensitivity to initial conditions and is characterised by one positive Lyapunov exponent, while others are hyperchaotic as introduced by [51] Rösler and is characterised by at least two positive Lyapunov exponents, generally with complex dynamical behaviours with much wider application. The literature on hyperchaotic models is recent and investigations on the topic are still ongoing. In this dissertation a four-dimensional hyperchaotic model consisting of two equilibrium points is investigated and analysed using the non-local and non-singular kernel operator. The numerical simulations are then presented. Furthermore, we develop a two step Adams-Bashforth numerical scheme in Laplace transform [22] that is used to solve integer order and non-integer order four-dimensional differential equations. Our primary goal is to show that the developed method is hyperchaotic. In addition, the error analysis of the method is presented and show that the method converges. The numerical simulations of the method applied to the four-dimensional model, Caputo-Lu-Chen model and the partial differential equation (wave equation) are presented.

Preliminary concepts necessary for the development of the Laplace Adams-Bashforth numerical scheme are presented. These among others include definitions, theorems and some properties of Laplace transform. The multistep Adams-Bashforth explicit method and its related local error is also presented. Finally, a brief historical background of

fractional calculus and various definitions are presented.

The remaining part of the dissertation is organised as follows: In chapter 2 we introduce the preliminary concepts that form part of the development of the Laplace Adams-Bashforth method as it will be seen in the later chapters. In chapter 3, the four-dimensional hyperchaotic model is analysed. In chapter 4 the Laplace Adams-Bashforth numerical scheme is derived and the error analysis relating to the derived numerical scheme is presented. The whole of chapter 5 is devoted to numerical simulations of the method applied to Caputo-Lu-Chen model, four-dimensional model and partial differential equation. Chapter 6 is the conclusion.

Chapter 2

Laplace Transform and Inverse Transform. Fourth-Order Adams-Bashforth Technique.

2.1 Laplace Transform

2.1.1 Introduction

Laplace transform is an [60] integral transform useful in solving physical problems and in particular linear ordinary differential equations. It is also[1] used to solve partial fractional differential equations. The section starts by presenting definitions, theorems and some useful properties [8] of Laplace transform which are used when solving linear initial value problems. Furthermore, we also provide conditions sufficient for the existence of the method of Laplace transform.

One of the classic characteristic of Laplace transform [60] is its ability to convert the function $g(t)$ in its time domain to the function in frequency domain $G(s)$. The[60] finite integral of the form $\int_c^d \mathbf{T}(s,t)g(t)dt$, transforming the function $g(t)$ into some function $G(s)$ are considered. If $g(t)$ of the [60] integral transform is defined for $t \geq 0$, and the interval of integration is $[0,\infty]$, then $\int_0^\infty \mathbf{T}(s,t)g(t)dt$ can be defined to be the limit

$$\int_0^\infty \mathbf{T}(s,t)g(t)dt = \lim_{d\to\infty} \int_c^d \mathbf{T}(s,t)g(t)dt. \tag{2.1.1}$$

The integral is considered to converge or exist, provided the limit in (2.1.1) exists. There are cases where the limit diverges and does not exist.

Definition 2.1.1. *Let the function g be defined for $t \geq 0$, then the integral*

$$\mathcal{L}g(t) = \int_0^\infty e^{-st} g(t)dt \tag{2.1.2}$$

is regarded as the Laplace transform of g, only if the integral is convergent.

In many instances [32] the function $g(t)$, is restricted. Consider an example where $g(t)$ goes to nonzero as $t \to \infty$, then the integral converges only if $s > 0$. In cases [32] where s is complex, $s = Re(s) + iIm(s)$ with $e^{-st} = e^{Re(s)t}[\cos(Im(s)t) - i\sin(Im(s)t)]$, then it follows that $Re(s) > 0$, for the integral to converge.

Theorem 2.1.2 (**Table: Basic Transform Functions**).

$$\begin{cases} \mathcal{L}\{1\} = \dfrac{1}{s}, \\ \mathcal{L}\{t^n\} = \dfrac{n!}{s^{n+1}} \qquad n = 1, 2, 3, \cdots, \\ \mathcal{L}\{e^{at}\} = \dfrac{1}{s-a}, \\ \mathcal{L}\{\sin \omega t\} = \dfrac{\omega}{s^2+\omega^2}, \\ \mathcal{L}\{\cos \omega t\} = \dfrac{s}{s^2+\omega^2}, \\ \mathcal{L}\{\sinh \omega t\} = \dfrac{\omega}{s^2-\omega^2}, \\ \mathcal{L}\{\cosh \omega t\} = \dfrac{s}{s^2-\omega^2}, \\ \mathcal{L}\{\sin \omega t + \omega t \cos \omega t\} = \dfrac{2\omega s^2}{(s^2+\omega^2)^2}, \\ \mathcal{L}\{\sin \omega t - \omega t \cos \omega t\} = \dfrac{2\omega^3}{(s^2+\omega^2)^2} \end{cases}$$

We use [60] the definition 2.1.1 to compute the transform of $\mathcal{L}(1)$ and $\mathcal{L}(e^{\beta t})$ in the following example:

Example 2.1.3 (**Applying Definition 2.1.1**). *We Compute* $\mathcal{L}(1)$

$$\mathcal{L}(1) = \int_0^\infty e^{-st}(1)dt = \frac{-e^{-st}}{s}\bigg|_0^\infty = \frac{1}{s}, \qquad s > 0.$$

Example 2.1.4 (**Applying Definition 2.1.1**). *We Compute* $\mathcal{L}(e^{\beta t})$ *for* $s > \beta$,

$$\mathcal{L}(e^{\beta t}) = \int_0^\infty e^{-(s-\beta)t}dt = -\frac{1}{s-\beta}e^{-(s-\beta)t}\bigg|_0^\infty = \frac{1}{s-\beta}.$$

The Laplace transform [8] $\mathcal{L}(e^{\beta t})(s)$ is said to be undefined for $s \leq \beta$.

The function f is said [8] to be of exponential order if there exist positive numbers v and N such that

$$|f(t)| \leq Ne^{vt} \qquad \text{for all} \qquad t \geq 0. \tag{2.1.3}$$

The following is the sufficient condition for the existence of the Laplace transform as defined in the following theorem

Theorem 2.1.5. *Suppose that f is piecewise continuous on the interval $[0, \infty]$ and of exponential order with $|f(t)| \leq Ne^{vt}$ for all $t \geq 0$. Then $\mathcal{L}(f)(s)$ exists for all $s > v$.[8]*

Proof. We must show that for $s > v$

$$\mathcal{L}(f)(s) = \int_0^\infty f(t)e^{-st}dt < \infty.$$

With N and v, we have

$$\begin{aligned}\left| \int_0^\infty f(t)e^{-st}dt \right| \leq \int_0^\infty |f(t)|e^{-st}dt &\leq N \int_0^\infty e^{vt}e^{-st}dt \\ &= N \int_0^\infty e^{-(s-v)t}dt = \frac{N}{s-v} < \infty.\end{aligned}$$

■

The theorem [8] only provides the sufficient, but not the necessary conditions for the existence of Laplace transform.

Example 2.1.6 (Applying the piecewise continuous function theorem 2.1.5). *We evaluate [60] $\mathcal{L}\{f(t)\}$ where*

$$f(t) = \begin{cases} 0, & 0 \leq t < 3 \\ 2, & t \geq 3. \end{cases}$$

The [60] function f is defined as two pieces and we then express $\mathcal{L}\{f(t)\}$ as the sum of two integrals

$$\begin{aligned}\mathcal{L}\{f(t)\} = \int_0^\infty e^{-st}f(t)dt &= \int_0^3 e^{-st}(0)dt + \int_3^\infty e^{-st}(2)dt \\ &= 0 + \frac{2e^{-st}}{-s}\|_3^\infty \\ &= \frac{2e^{-3t}}{s}, \qquad s > 0.\end{aligned}$$

To conclude this section, we consider the theorem that shows that [60] not every arbitrary functions of s fulfil the conditions for the Laplace transform of a piecewise continuous function of exponential order.

Theorem 2.1.7 (Behaviour of $F(s)$ as $s \to \infty$)**.** *If f is piecewise continuous on $(0, \infty)$ and of exponential order and $F(s) = \mathcal{L}f(t)$, then $\lim_{s\to\infty} F(s) = 0$.*

For the proof, refer to [60].

Theorem 2.1.8. ***Linearity*** *[8] If f and g are functions and φ and ϕ are numbers, then*

$$\mathcal{L}(\varphi f + \phi g) = \varphi\mathcal{L}(f) + \phi\mathcal{L}(g). \tag{2.1.4}$$

For the proof, refer to [8]. Looking at some examples using the linearity theorem (2.1.8),we [8] evaluate $\mathcal{L}(\cos(ct))$ and $\mathcal{L}(\sin(ct))$ and base the example on the Euler's identity $e^{ict} = \cos(ct) + i\sin(ct)$. The linearity of the Laplace transform of the identity will take the form as in the following example

Example 2.1.9 (Evaluate $\mathcal{L}(\cos(ct))$ **and** $\mathcal{L}(\sin(ct))$)**.**

$$\begin{aligned}
\mathcal{L}(\cos(ct)) + i\mathcal{L}(\sin(ct)) &= \int_0^\infty (\cos(ct) + i\sin(ct))e^{-st}dt = \int_0^\infty e^{ict}e^{-st}dt \\
&= \int_0^\infty e^{-t(s-ic)}dt \\
&= -\frac{e^{-t(s-ic)}}{s-ic}\Big|_0^\infty = \frac{1}{s-ic} \\
&= \frac{s+ic}{s^2+c^2} \\
&= \frac{s}{s^2+c^2} + i\frac{c}{s^2+c^2}.
\end{aligned}$$

Equating the real and the imaginary parts, we have

$$\mathcal{L}(\cos(ct)) = \frac{s}{s^2+c^2} \qquad \textit{and} \qquad \mathcal{L}(\sin(ct)) = i\frac{c}{s^2+c^2}.$$

2.1.2 Transforms of Derivatives

Laplace transforms are [60] mainly used to solve differential equations such as $\mathcal{L}\{dx/dt\}$ and $\mathcal{L}\{d^2x/dt^2\}$. These types of Laplace transforms of derivatives are recursive in nature. The nth derivatives of f of the Laplace transform is given in the following theorem.

Theorem 2.1.10. ***Laplace Transforms of Derivatives*** *[8] Suppose that f is continuous on $[0, \infty)$ and of exponential order as given in equation* (2.1.3)*. Suppose further*

that f' is piecewise continuous on $[0,\infty)$ and of exponential order. Then

$$\mathcal{L}(f') = s\mathcal{L}(f) - f(0). \tag{2.1.5}$$

More generally, if $f, f', ..., f^{(n-1)}$ are continuous on $[0,\infty)$ and of exponential order, and if $f^{(n)}$ is piecewise continuous on $(0,\infty)$ and of exponential order, then

$$\mathcal{L}(f^{(n)}) = s^n\mathcal{L}(f) - s^{n-1}f(0) - s^{n-2}f'(0) - ... - f^{(n-1)}(0). \tag{2.1.6}$$

The Laplace transform takes the powers of t into the derivatives as shown in the following theorem:

Theorem 2.1.11. ***Derivatives of Transforms*** *[8] Suppose f is piecewise continuous and of equation of exponential order. Then*

$$\mathcal{L}(tf(t))(s) = -\frac{d}{ds}\mathcal{L}(f)(s). \tag{2.1.7}$$

In general, if $f(t)$ is piecewise continuous and of exponential order, then

$$\mathcal{L}(t^n f(t)) = (-1)^n \frac{d^n}{ds^n}\mathcal{L}(f)(s). \tag{2.1.8}$$

Proof.

$$\begin{aligned}\mathcal{L}(f)t'(s) =& \frac{d}{ds}\int_0^\infty f(t)e^{-st}dt = \int_0^\infty f(t)\frac{d}{ds}e^{-st}dt \\ =& -\int_0^\infty tf(t)e^{-st}dt = -\mathcal{L}(tf(t))(s).\end{aligned}$$

■

2.1.3 Transform of Integrals

Let f and g be the [60] piecewise continuous functions on the interval $[0,\infty,]$ the the product $f * g$ defined by the integral

$$f * g = \int_0^t f(\varphi)g(t-\varphi)d\varphi \tag{2.1.9}$$

is called the convolution of f and g.

Theorem 2.1.12 (**Convolution Theorem**). *[60] if $u(t)$ and $v(t)$ are piecewise con-*

tinuous on $[0,\infty]$ *and of exponential order, then*

$$\mathcal{L}\{u*v\} = \mathcal{L}\{u(t)\}\mathcal{L}\{v(t)\} = U(s)V(s).$$

Proof. Let

$$U(s) = \mathcal{L}\{u(t)\} = \int_0^\infty e^{-s\varphi}u(\varphi)d\varphi$$

and

$$V(s) = \mathcal{L}\{v(t)\} = \int_0^\infty e^{-s\alpha}v(\alpha)d\alpha.$$

thus:

$$\begin{aligned} U(s)V(s) =& \left(\int_0^\infty e^{-s\varphi}u(\varphi)d\varphi\right)\left(\int_0^\infty e^{-s\alpha}v(\alpha)d\alpha\right) \\ =& \int_0^\infty\int_0^\infty e^{-s(\varphi+\alpha)}u(\varphi)v(\alpha)d\varphi d\alpha \\ =& \int_0^\infty u(\varphi)d\varphi\int_0^\infty e^{-s(\varphi+\alpha)}v(\alpha)d\varphi. \end{aligned}$$

Holding φ fixed, and we let $t = \varphi+\alpha, dt = d\alpha$, so that

$$U(s)V(s) = \int_0^\infty u(\varphi)d\varphi\int_0^\infty e^{-st}v(t-\varphi)dt.$$

Since u and v are piecewise continuous on $[0,\infty]$ and of exponential order, it is possible to interchange the order of integration:

$$U(s)V(s) = \int_0^\infty e^{-st}\int_0^\infty u(\varphi)v(t-\varphi)dt = \int_0^\infty e^{-st}\left\{\int_0^\infty u(\varphi)v(t-\varphi)d\varphi\right\}dt = \mathcal{L}\{u*v\}.$$

■

To apply or demonstrate the foregoing, an example in [60] is adopted, and $\mathcal{L}\left\{\int_0^t e^{\varphi}\sin(t-\varphi)d\varphi\right\}$ is evaluated with $u(t) = e^t$ and $v(t) = \sin(t)$, and have

Example 2.1.13 (**Transform of a Convolution**)**.**

$$\mathcal{L}\left\{\int_0^t e^{\varphi}\sin(t-\varphi)d\varphi\right\} = \mathcal{L}\{e^t\}\cdot\mathcal{L}\{\sin t\} = \frac{1}{s-1}\cdot\frac{1}{s^2+1} = \frac{1}{(s-1)(s^2+1)}.$$

2.1.4 Translation on the s-Axis

It is easy to compute the Laplace transform of an exponential multiple of f, which is $\mathcal{L}\{e^{-s}f(t)\}$ when we know the Laplace transform of f. To achieve this we translate or shift the transform $F(s)$ to $F(s-a)$ and that is known as the first translation theorem

or the first shifting theorem.

Theorem 2.1.14. ***First Translation Theorem*** *If $\mathcal{L}\{f(t)\} = F(s)$ and a is any real number, then*

$$\mathcal{L}\{f(t)\} = F(s-a).$$

For the full proof, refer to [60].

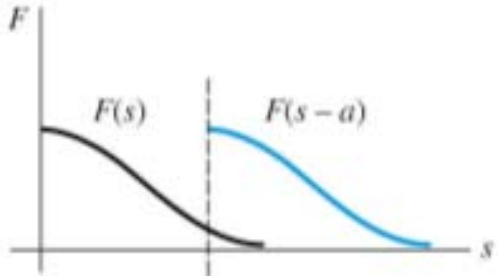

Figure 2.1: $s = a, a > 0$ shift on s-axis

Considering the real variable s in figure (2.1), then the graph of $F(s-a)$ is the representation of graph $F(s)$ shifted by the magnitude of $|a|$ on the s-axis. Now, [32] depending on the value of a, we have that the graph of $F(s)$ is shifted a units to the right if $a > 0$, otherwise is shifted $|a|$ units to the left if $a < 0$.

Example 2.1.15. ***Using the First Translation Theorem*** *to evaluate $\mathcal{L}\{e^{5t}t^3\}$ we have*

$$\mathcal{L}\{e^{5t}t^3\} = \mathcal{L}\{t^3\}\Big|_{s\to s-5} = \frac{3!}{s^4}\Big|_{s\to s-5} = \frac{6}{(s-5)^4}.$$

2.1.5 Singularities of the Laplace Transform

We first consider the [32] simple exponential function $f(t) = e^{rt}$ where the growth rate r is the point where its Laplace transform $F(s) = \dfrac{1}{s-r}$ has a singularity or roots. We also note that as $s \to r$, the Laplace transform $F(s)$ approaches ∞. The roots or singularities of a Laplace transform $F(s)$ have a direct relationship with the growth rate $f(t)$, [32] and this is referred to as the singularity property of Laplace transform. Let us consider an example using the partial fraction method.

Example 2.1.16. *Evaluate the Laplace transform $F(s) = \dfrac{3}{[s(s^2+4)]}$.*

$$\frac{3}{s(s^2+4)} = \frac{A}{s} + \frac{Bs+C}{s^2+4} = \frac{3/4}{s} + \frac{-(3/4)s}{s^2+4}.$$

and the inverse transform is solved by using the table

$$f(t) = \frac{3}{4} - \frac{3}{4}\cos 2t.$$

2.1.6 Partial Fractions

In most cases when [32] we work with inverse Laplace transform, the ratio of two polynomials of the form $g(s)/h(s)$ is involved. The Laplace transform, $g(s)/h(s)$ must approach 0 as $s\to\infty$, assuming that the degree of h is greater than the degree of g. To achieve the [32] inverse Laplace transform, we first must factor the denominator $h(s)$, and doing this yields

$$h(s) = \beta(s - s_1)(s - s_2)\cdots(s - s_n),$$

where $s_1, \cdots, s_n$ are the n distinct roots of $h(s)$. The expansion of the partial fraction $g(s)/h(s)$ then is

$$\frac{g(s)}{h(s)} = \frac{k_1}{s - s_1} + \frac{k_2}{s - s_2} + \cdots + \frac{k_n}{s - s_n}. \tag{2.1.10}$$

We need to determine the [32] coefficient k_i of the partial fraction expansion using the singularities k_i of $g(s)/h(s)$. This is achieved by multiplying (2.1.10) by $s - s_i$ and then [32] taking the limit as $s\to s_i$ thus

$$k_i = \lim_{s\to s_i} \frac{(s - s_i)g(s)}{h(s)}. \tag{2.1.11}$$

We consider an example using complex roots to evaluate $\dfrac{3}{s(s^2+4)}$ and we have

$$\frac{3}{s(s^2+4)} = \frac{k_1}{s} + \frac{k_2}{s+2i} + \frac{k_3}{s-2i},$$

where

$$\begin{aligned}
k_1 &= \lim_{s\to 0} s\frac{3}{s(s^2+4)} = \frac{3}{4}\\
k_2 &= \lim_{s\to -2i}(s+2i)\frac{3}{s(s^2+4)} = \lim_{s\to -2i}(s+2i)\frac{3}{s(s+2i)(s-2i)} = -\frac{3}{8}\\
k_3 &= \lim_{s\to 2i}(s-2i)\frac{3}{s(s^2+4)} = \lim_{s\to 2i}(s-2i)\frac{3}{s(s+2i)(s-2i)} = -\frac{3}{8}.
\end{aligned}$$

We have that[32] the limit in (2.1.11) is 0/0 since $h(s_i) = 0$. This is because $s = s_i$ is the root of $h(s)$. We use L'Hôpital's rule for evaluating 0/0 and we have

$$k_i = \lim_{s \to s_i} \frac{\frac{d}{ds}[(s - s_i)g(s)]}{\frac{d}{ds}h(s)} = \frac{g(s_i)}{h'(s_i)}. \tag{2.1.12}$$

The inverse transform can thus easily be obtained from a partial fraction expansion of a Laplace transform and is summarised [32] as follows. If

$$F(s) = \frac{g(s)}{h(s)}, \tag{2.1.13}$$

then inverting equation (2.1.10) gives

$$f(t) = \sum_{i=1}^{n} \frac{g(s_i)}{h'(s_i)} e^{es_i t}, \tag{2.1.14}$$

assuming that $h(s)$ has simple roots at $s = s_i$.
The formula above can be applied for $\frac{g(s)}{h(s)} = \frac{3}{[s(s^2+4)]}$,
we set $g(s) = 3$ and $h(s) = s(s^2 + 4)$. First, we determine $h'(s) = 3s^2 + 4$. If

$$F(s) = \frac{3}{s(s^2+4)} = \frac{k_1}{s} + \frac{k_2}{s+2i} + \frac{k-3}{s-2i},$$

then, we have

$$\begin{aligned} k_1 &= \frac{g(0)}{h'(0)} = \frac{3}{4}, \\ k_2 &= \frac{g(-2i)}{h'(-2i)} = -\frac{3}{8}, \\ k_3 &= \frac{g(2i)}{h'(2i)} = -\frac{3}{8}. \end{aligned}$$

For this example, we have

$$f(t) = \frac{3}{4} - \frac{3}{8}e^{2it} - \frac{3}{8}e^{2it} = \frac{3}{4} - \frac{3}{4}\cos 2t.$$

2.1.7 Translation on the t-Axis

These are unit step functions normally used [60] in the field of engineering for representing systems that switches between on and off. We consider [8] a function $f(t)$ that

represents a signal, then $\mathcal{U}_0(t-a)f(t-a)$ is the representation of the same signal delayed by a unit of time.

Theorem 2.1.17. ***Second Translation Theorem.***
If a is a positive real number, then

$$\mathcal{L}(\mathcal{U}_0(t-a)f(t-a))(s) = e^{-st}F(s),$$

where $F(s) = \mathcal{L}(f(t))(s)$.

Proof. By the additive interval property of integrals,

$$\int_0^\infty f(t-a)\mathcal{U}(t-a)e^{-st}dt$$

can be written as the sum of two integrals:

$$\mathcal{L}\{f(t-a)\mathcal{U}(t-a)\} = \int_0^a f(t-a)\mathcal{U}(t-a)e^{-st}dt + \int_a^\infty f(t-a)\mathcal{U}(t-a)e^{-st}dt = \int_a^\infty f(t-a)e^{-st}dt.$$

Now, let $r = t-a, dr = dt$ in the last integral, then

$$\mathcal{L}\{f(t-a)\mathcal{U}(t-a)\} = \int_0^\infty f(r)e^{-s(r+a)}dr = e^{-as}\int_0^\infty e^{-sr}f(r)dr = e^{-as}\mathcal{L}\{f(t)\}.$$

■

2.2 Inverse Transform

The inverse of a Laplace transform $h\mathcal{L}^{-1}$ is a linear transform that [60] converts a function $F(s)$ from its frequency domain to the time domain function $f(t)$ and is defined by

$$f(t) = \mathcal{L}^{-1}(F(s))$$

An illustration of [60] the definition with 2.1.3 and 2.1.4 in section 2.1 we have, respectively

Inverse transform examples	
$\mathcal{L}\{1\} = \frac{1}{s}$	$1 = \mathcal{L}^{-1}\left\{\frac{1}{s}\right\}$
$\mathcal{L}\{e^{-\beta t}\} = \frac{1}{s+\beta}$	$e^{-\beta t} = \mathcal{L}^{-1}\left\{\frac{1}{s+\beta}\right\}$

The inverse [8] of linear transform is also itself linear, as shown in the linear equation below

$$\mathcal{L}^{-1}(\varphi F + \phi G) = \varphi\mathcal{L}^{-1}(F) + \phi\mathcal{L}^{-1}(G),$$

where F and G are [60] transforms of some functions f and g.

Example 2.2.1. ***linearity***

$$\begin{aligned}\mathcal{L}^{-1}\left\{\frac{-2s+6}{s^2+4}\right\} =& \mathcal{L}^{-1}\left\{\frac{-2s}{s^2+4} + \frac{6}{s^2+4}\right\} = -2\mathcal{L}^{-1}\left\{\frac{s}{s^2+4}\right\} + \frac{6}{2}\mathcal{L}^{-1}\left\{\frac{2}{s^2+4}\right\} \\ =& -2\cos 2t + 3\sin 2t.\end{aligned}$$

In the previous section 2.1 we outlined the translation theorem on the s-Axis in theorem (2.1.14). The [60] inverse form of the theorem can be represented by

$$\mathcal{L}^{-1}\{F(s-a)\} = \mathcal{L}^{-1}\{F(s)\Big|_{s\to s-a}\} = e^{st}f(t),$$

where $f(t) = \mathcal{L}^{-1}\{F(s)\}$.

The inverse form of [60] Theorem 2.1.17 is defined as

Definition 2.2.2. *if $f(t) = \mathcal{L}^{-1}\{F(s)\}$, the inverse form of Theorem 2.1.17, $a > 0$, is*

$$\mathcal{L}^{-1}\{e^{-as}F(s)\} = f(t-a)\mathcal{U}(t-a). \tag{2.2.1}$$

The [60] inverse form of Theorem 2.1.9 has the form

$$\mathcal{L}^{-1}\{F(s)G(s) = f * s\}.$$

using [60] $\mathcal{L}\{\sin\omega t + \omega t\cos\omega t\} = \dfrac{2\omega^3}{(s^2+\omega^2)^2}$ entry from Theorem 2.1.2 to evaluate $\mathcal{L}^{-1}\left\{\dfrac{1}{(s^2+\omega^2)^2}\right\}$, and Let $F(s) = G(s) = \dfrac{1}{s^2+\omega^2}$, then

Example 2.2.3 (**Inverse transform as a Convolution**).

$$f(t) = g(t) = \frac{1}{\omega^2}\mathcal{L}^{-1}\left\{\frac{\omega}{s^2+\omega^2}\right\} = \frac{1}{\omega}\sin\omega t.$$

Using equation (2.2)*, we have*

$$\mathcal{L}^{-1}\left\{\frac{1}{(s^2+\omega^2)^2}\right\} = \frac{1}{\omega^2}\int_0^t \sin\omega\varphi\sin\omega(t-\varphi)d\varphi. \tag{2.2.2}$$

Now, using the trigonometric identity

$$\sin\alpha\cos\beta = \frac{1}{2}[\cos(\alpha-\beta)-\cos(\alpha+\beta)]$$

and substituting $\alpha = \omega\varphi$ *and* $\beta = \omega(t-\varphi)$ *the integration in* (2.2.2) *becomes:*

$$\begin{aligned}\mathcal{L}^{-1}\left\{\frac{1}{(s^2+\omega^2)^2}\right\} =& \frac{1}{s\omega^2}\int_0^t [\cos\omega(2\varphi-t)-\cos\omega t]d\varphi \\ =& \frac{1}{2\omega^2}\left[\frac{1}{s\omega}\sin\omega(2\varphi-t)-\varphi\cos\omega t\right]_0^t \\ =& \frac{\sin\omega t-\omega t\cos\omega t}{2\omega^3}.\end{aligned}$$

Multiplying both sides by $2\omega^3$ *gives the inverse form* $\mathcal{L}\{\sin\omega t+\omega t\cos\omega t\} = \dfrac{2\omega^3}{(s^2+\omega^2)^2}$.

2.3 Adams-Bashforth Explicit Methods

The Adams-Bashforth method is [22] recognised to be the powerful tool to solve partial differential equations with classical derivatives and differential equations with non-integer order derivatives. This numerical scheme is applied in [22] many fields of applied science, engineering epidemiology and in chaotic problems.

The [48, 21, 41, 20] Adams-Bashforth method is one of the multistep numerical schemes that use the approximation at more than one previous mesh point to determine the approximation at the next point and it is defined as [48]

Definition 2.3.1. *An* ***r-step multistep method*** *for solving the initial-value problem*

$$y' = z(\tau, y), a \le \tau \le b, y(a) = \beta, \tag{2.3.1}$$

has a difference equation for finding the approximation u_{j+1} *at the mesh point* t_{j+1} *represented by the following equation, where* r *is an integer greater than 1:*

$$\begin{aligned}&u_{j+1} = a_{r-1}u_j + a_{r-2}u_{j-1} + ... + a_0u_{j+1-r} \\ &+h[b_rz(t_{j+1},u_{j+1})] + b_{r-1}z(t_j,u_j) \\ &+... + b_0z(t_{j+1-r},u_{j+1-r})],\end{aligned} \tag{2.3.2}$$

for $j = r-1, r, ..., N-1$, *where* $h = (b-a)/N$, *the* $a_0, a_1, \cdots, a_{r-1}$ *and* $b_0, b_1, \cdots, b_r$ *are constants, and the starting values*

$u_0 = \beta, u_1 = \beta_1, u_2 = \beta_2, \cdots, u_{r-1} = \beta_{r-1}$
are specified.

The derivation [48] of this multistep method begins with solution to the initial-value problem

$$y' = z(\tau, y), a \leq \tau \leq b, y(a) = \beta,$$

integrating over the interval $[\tau_j, \tau_{j+1}]$ gives the property

$$y(\tau_{j+1}) - y(\tau_j) = \int_{\tau_j}^{\tau_{j+1}} y'(\tau) d\tau = \int_{\tau_j}^{\tau_{j+1}} z(\tau, y(\tau)) d\tau.$$

and hence,

$$y(\tau_{j+1}) = y(\tau_j) + \int_{\tau_j}^{\tau_{j+1}} z(\tau, y(\tau)) d\tau. \tag{2.3.3}$$

If we [48] integrate an interpolating polynomial $L(\tau)$ to $z(\tau, y(\tau))$, determined by previous data points $(\tau_0, u_0, (\tau_1, u_1), \cdots, (\tau_j, u_j))$, and further assume that $y(\tau_j) \approx u_j$ then equation (2.3.3) becomes

$$y(\tau_{j+1}) \approx u_j + \int_{\tau_j}^{\tau_{j+1}} L(\tau) d\tau. \tag{2.3.4}$$

Using the [48] backward-difference polynomial $L_{r-1}(\tau)$ through to derive the Adams-Bashforth explicitly, we have

$$(\tau_j, z(\tau_j, y(\tau_j))), (\tau_{j-1}, z(\tau_{j-1}, y(\tau_{j-1}))), ..., (\tau_{j+1-m}, z(\tau_{j+1-m}, y(\tau_{j+1-m}))).$$

We have the [48] polynomial $L_{r-1}(\tau)$ of degree $r-1$ and it has some number ξ_j in (τ_{j+1-r}, τ_j) that exists with

$$z(\tau, y(\tau)) = L_{r-1}(\tau) + \frac{z^{(r)}(\xi_j, y(\xi_j))}{r!}(\tau - \tau_j)(\tau - \tau_{j-1}) \cdots (\tau - \tau_{j+1-r}).$$

By changing [48] the variable substitution $\tau = \tau_j + sh$, with $d\tau = h\ ds$, into $L_{r-1}(\tau)$

and the error term implies that

$$\begin{aligned}\int_{\tau_j}^{\tau_{j+1}} z(\tau, y(\tau)) =& \int_{\tau_j}^{\tau_{j+1}} \sum_{l=0}^{r-1} (-1)^l \binom{-s}{l} \nabla^l z(\tau_j, y(\tau_j)) \\ &+ \int_{\tau_j}^{\tau_{j+1}} \frac{z^{(r)}(\xi_j, y(\xi_j))}{r!} (\tau - \tau_j)(\tau - \tau_{j-1}) \cdots (\tau - \tau_{j+1-r}) d\tau \\ =& \sum_{l=0}^{r-1} \nabla^l z(\tau_j, y(\tau_j)) h (-1)^l \int_0^1 \binom{-s}{l} ds \\ &+ \frac{h^{r+1}}{r!} \int_0^1 s(s+1) \cdots (s+r-1) z^{(r)}(\xi_j, y(\xi_j)) ds.\end{aligned}$$

Setting [48] the value $l = 0, 1, \cdots, 5$ in the integral $(-1)^l \int_0^1 \binom{-s}{l} ds$, we have for $l = 0$,

$$(-1)^0 \int_0^1 \binom{-s}{0} ds = -\int_0^1 \frac{(s)}{0!} ds = -\int_0^1 1 ds = 1.$$

For $l = 1$, we have

$$(-1)^1 \int_0^1 \binom{-s}{1} ds = -\int_0^1 \frac{(-s)}{1} ds = -\int_0^1 (-s) ds = \frac{1}{2}.$$

For $l = 2$, we have

$$(-1)^2 \int_0^1 \binom{-s}{2} ds = -\int_0^1 \frac{(s)(-s-1)}{2 \cdot 1} ds = -\frac{1}{2} \int_0^1 (-s^2 - s) ds = \frac{5}{12}.$$

For $l = 3$, we have

$$\begin{aligned}(-1)^3 \int_0^1 \binom{-s}{3} ds =& -\int_0^1 \frac{(-s)(-s-1)(-s-2)}{3 \cdot 2 \cdot 1} ds \\ =& \frac{1}{6} \int_0^1 (s^3 + 3s^2 + 2s) ds \\ =& \frac{1}{6} \left[\frac{s^4}{4} + s^3 + s^2 \right]_0^1 = \frac{1}{6} \left(\frac{9}{4} \right) = \frac{3}{8}.\end{aligned}$$

Consequently [48], we have

$$\begin{aligned}\int_{\tau_j}^{\tau_{j+1}} z(\tau, y(\tau)) d\tau =& h \left[z(\tau_j, y(\tau_j)) + \frac{1}{2} \nabla z(\tau_j, y(\tau_j)) + \frac{5}{12} \nabla^2 z(\tau_j, y(\tau_j)) + \cdots \right] \\ &+ \frac{h^{r+1}}{r!} \int_0^1 s(s+1) \cdots (s+r-1) z^{(r)}(\xi_j, y(\xi_j)) ds.\end{aligned} \tag{2.3.5}$$

Since [48] $s(s+1)\cdots(s+r-1)$ is not changing sign on $[0,1]$, we can use the Weighted Mean Value Theorem for Integral to deduce that for some numbers μ_j, where $\tau_{j+1-r<\mu_j<\tau_{j+1}}$, the error term in equation (2.3.5) then becomes

$$\begin{aligned}\frac{h^{r+1}}{r!}\int_0^1 s(s+1)\cdots(s+r-1)z^{(r)}(\xi_j,y(\xi_j))ds\\ =\frac{h^{r+1}z^{(r)}(\mu_j,y(\mu_j))}{r!}\int_0^1 s(s+1)\cdots(s+r-1)ds.\end{aligned}$$

The error term [48] in equation (2.3.5) can be simplified to

$$h^{r+1}z^{(r)}(\mu_j,y(\mu_j))(-1)^r\int_0^1\binom{-s}{r}ds. \tag{2.3.6}$$

But we have [48] that $y(\tau_{j+1})-y(\tau_j)=\int_{\tau_j}^{\tau_{j+1}}z(\tau,y(\tau))d\tau$, and hence equation (2.3.3) can be written as

$$\begin{aligned}y(\tau_{j+1}) =&y(\tau_j)+h\left[z(\tau_j,y(\tau_j))+\frac{1}{2}\nabla z(\tau_j,y(\tau_j))+\frac{5}{12}\nabla^2 z(\tau_j,y(\tau_j))+\cdots\right]\\ &+h^{r+1}z^{(r)}(\mu_j,y(\mu_j))(-1)^r\int_0^1\binom{-s}{r}ds.\end{aligned} \tag{2.3.7}$$

In order to derive [48] the third-order Adams-Bashforth technique, we set $r=3$ in equation (2.3.7) and we have

$$\begin{aligned}y(\tau_{j+1}) \approx&y(\tau_j)+\int_{\tau_j}^{\tau_{j+1}}\sum_{l=0}^{r-1}(-1)^l\binom{-s}{l}\nabla^l z(\tau_j,y(\tau_j))hds\\ =&y(\tau_j)+\sum_{l=0}^{2}\nabla^l z(\tau_j,y(\tau_j))h(-1)^l\int_0^1\binom{-s}{l}ds\\ =&y(\tau_j)+h\left[z(\tau_j,y(\tau_j))+\frac{1}{2}\nabla z(\tau_j,y(\tau_j))+\frac{5}{12}z(\tau_j,y(\tau_j))\right]\\ =&y(\tau_j)+h\Big\{z(\tau_j,y(\tau_j))+\frac{1}{2}[z(\tau_j,y(\tau_j))-z(\tau_{j-1},y(\tau_{j-1}))]\\ &+\frac{5}{12}[z(\tau_j,y(\tau_j))-2z(\tau_{j-1},y(\tau_{j-1}))+z(\tau_{j-2},y(\tau_{j-2}))]\Big\}\\ =&y(\tau_j)+\frac{h}{12}[23z(\tau_j,y(\tau_j))-16z(\tau_{j-1},y(\tau_{j-1}))+5z(\tau_{j-2},y(\tau_{j-2}))].\end{aligned}$$

Similarly we can derive the fourth-order Adams-Bashforth by setting $r=4$ in equation

(2.3.7)

$$
\begin{aligned}
y(\tau_{j+1}) \approx & y(\tau_j) + \int_{\tau_j}^{\tau_{j+1}} \sum_{l=0}^{m-1} (-1)^l \binom{-s}{l} \nabla^l z(\tau_j, y(\tau_j)) h ds \\
= & y(\tau_j) + \sum_{l=0}^{3} \nabla^l z(\tau_j, y(\tau_j)) h (-1)^l \int_0^1 \binom{-s}{l} ds \\
= & y(\tau_j) + h\left[z(\tau_j, y(\tau_j)) + \frac{1}{2}\nabla z(\tau_j, y(\tau_j)) + \frac{5}{12} z(\tau_j, y(\tau_j)) + \frac{3}{3} z(\tau_j, y(\tau_j)) \right] \\
= & y(\tau_j) + h\Big\{ z(\tau_j, y(\tau_j)) + \frac{1}{2}[z(\tau_j, y(\tau_j)) - z(\tau_{j-1}, y(\tau_{j-1}))] \\
& + \frac{5}{12}[z(\tau_j, y(\tau_j)) - 2z(\tau_{j-1}, y(\tau_{j-1})) + z(\tau_{j-2}, y(\tau_{j-2}))] \Big\} \\
& + \frac{3}{8}[z(\tau_j, y(\tau_j)) - 3z(\tau_{j-1}, y(\tau_{j-1})) + 3z(\tau_{j-2}, y(\tau_{j-2})) - z(\tau_{j-3}, y(\tau_{j-3}))] \\
= & y(\tau_j) + \frac{h}{24}[55z(\tau_j, y(\tau_j)) - 59z(\tau_{j-1}, y(\tau_{j-1})) + 37z(\tau_{j-2}, y(\tau_{j-2})) - 9z(\tau_{j-3}, y(\tau_{j-3}))].
\end{aligned}
$$

The following are some of the [48] explicit multistep methods and their required starting values. The associated local truncation errors are also presented.

Adams-Bashforth Two-Step explicit method

The two step Adams-Bashforth [48] is an explicit method with the starting value and local truncation error, and is defined as

$$
\begin{aligned}
& u_0 = \beta, u_1 = \beta_1, \\
& u_{j+1} = w_j + \frac{h}{2}[3z(\tau_j, u_j) - z(\tau_{j-1}, u_{j-1})],
\end{aligned} \tag{2.3.8}
$$

where $j = 1, 2, ..., N-1$. The local truncation error is $\rho_{j+1}(h) = \frac{5}{12} y'''(\mu_j) h^2$, for some $\mu_j \in (\tau_{j-1}, \tau_{j+1})$.

Adams-Bashforth Three-Step explicit method

The three-step explicit method is [48] defined to be

$$
u_0 = \beta, u_1 = \beta_1, u_2 = \beta_2,
$$

$$u_{j+1} = u_j + \frac{h}{12}[23z(\tau_j, u_j) - 16z(\tau_{j-1}, u_{j-1}) + 5z(\tau_{j-2}, u_{j-2})], \qquad (2.3.9)$$

where $j = 2, 3, ..., N-1$. The local truncation error is $\rho_{j+1}(h) = \frac{3}{8}y^{(4)}(\mu_j)h^3$, for some $\mu_j \in (\tau_{j-2}, \tau_{j+1})$.

Adams-Bashforth Four-Step explicit method

Similarly [48], the four-step explicit method is defined as

$$\begin{aligned} &u_0 = \beta, u_1 = \beta_1, u_2 = \beta_2, u_2 = \beta_3, \\ &u_{j+1} = u_j + \frac{h}{24}[55z(\tau_j, u_j) - 59z(\tau_{j-1}, u_{j-1}) \\ &+37z(\tau_{j-2}, u_{j-2}) - 9z(\tau_{j-3}, u_{j-3})], \end{aligned} \qquad (2.3.10)$$

where $j = 3, 4, ..., N-1$. The local truncation error is $\rho_{j+1}(h) = \frac{251}{720}y^{(5)}(\mu_j)h^4$, for some $\mu_j \in (\tau_{j-3}, \tau_{j+1})$.

2.4 Multistep Method Local Error

The multistep method [48] provides us with the necessary measure that must indicate how the solution to the differential equation method fails to solve the difference equation. This brings us to multistep local truncation error that is defined similarly with the one-step method truncation error.

Definition 2.4.1. *If y(t) is the solution to the initial-value problem*

$$y' = z(\tau, y), \qquad a \le \tau \le b, \qquad y(a) = \beta$$

and

$$\begin{aligned} u_{j+1} =& a_{r-1}u_j + a_{r-2}u_{j-1} + \cdots a_0 u_{j+1-r} \\ &+h\Big[b_r z(t_{j+1}, u_{j+1} + b_{r-1}z(\tau_j, u_j) + \cdots + b_0 z(\tau_{j+1-r}, y(\tau_{j+1-r}))\Big] \end{aligned}$$

is the $(j+1)$st step in a multistep method, the ***local truncation error*** *at this step is*

$$\begin{aligned} \chi_{j+1}(h) =& \frac{y(\tau_{j+1} - a_{r-1}y(\tau_j) - \cdots - a_0 y(\tau_{j+1-r})}{h} \\ &-h\Big[b_r z(\tau_{j+1}, u_{j+1} + b_{r-1}z(\tau_j, u_j) + \cdots + b_0 z(\tau_{j+1-r}, y(\tau_{j+1-r}))\Big], \end{aligned} \qquad (2.4.1)$$

for each $j = r-1, r, \cdots, N-1$.

Chapter 3

Four-Dimensional Hyperchaotic systems

3.1 Introduction

In this chapter we consider the four-dimensional hyperchaotic system and briefly outline some of its basic dynamics. Chaos [19, 11] is a nonlinear phenomenon known for its extreme sensitivity to initial condition and is characterised by one positive Lyapunov exponent. The first chaotic attractor was discovered in 1963 by Lorenz [19, 57] since then, extensive studies have been made in the field of mathematics, physics and engineering. Other three dimensional chaotic systems were proposed [36, 59, 46, 52, 31, 23] based on the Lorenz system and they are: Chen and Lü chaotic systems. On the other hand, hyperchaos was introduced by [51, 12, 55] Rössler in the ordinary differential equations and is mainly characterised by at least two Lyapunov exponents or equilibrium points, generally with complex dynamical behaviours and much wider application.

In the analysis of the four-dimensional hyperchaotic model, we will look into the chaotic nature of the model, its symmetry and the two unstable Lyapunov exponents using fractional calculus. We will also study [28] attractors, in particular strange attractors [28] that exists when the non-singular kernel and non-local operators are applied to the 4-dimensional hyperchaotic model. Dynamical systems possessing chaotic attractors normally are locally unstable and yet globally stable as they form an attractor. The numerical simulations that show the existence of these strange attractors will be done and provided in the study.
Before we proceed with our analysis, we need to define a useful new derivative operator

and its associated anti-derivative necessary for the analysis of the model.

The [28, 5] new fractional derivative with non-local and non-local kernel suggested by Atangana-Baleanu in Caputo sense which is commonly known as ABC, of order ϕ, with $0 < \phi \leq 1$ is defined by

$$ {}^{ABC}D_t^{\phi} f(t) = \frac{W(\phi)}{(1-\phi)} \int_0^t f'(\varphi) E_{\phi}\Big[-\phi \frac{(t-\varphi)^{\phi}}{(1-\phi)} \Big] d\varphi. \tag{3.1.1} $$

The [28] associated integral of the ABC is given by

$$ {}^{AB}J_t^{\phi} f(t) = \frac{\phi}{W(\phi)\Gamma(\phi)} \int_0^t (t-\varphi)^{\phi-1} f(\varphi) d\varphi + \frac{1-\phi}{W(\phi)} f(t), \qquad t > 0. \tag{3.1.2} $$

3.2 Fractional Derivatives

3.2.1 Brief Historical Background

Differential equations [34, 5, 25, 6, 15, 39] with integer order and those of non-integer order are mainly used to describe, model and analyse complex problems in engineering and science in general. Some of the examples include control theory, acoustics, viscoelasticity, image processing, acoustic dissipation, bioengineering, secure communication. Researchers in recent years have come to realise that fractional differential equations with fractional order are [42, 18, 26, 47, 17, 54] the most efficient and valuable tools to describe complex problem in real life in comparison with integer order differential equations. Historically, the fractional calculus concept is as old as the integer order derivatives concept, and is said to have been born out of a question put forward in a letter written [44, 38, 43] in 1695 by G. W. Leibniz. In the letter, G. W. Leibniz asked Marquis de l'Hopital specifically about a notation he had used in his publication for the nth-derivative of a linear function defined by $g(x) = x, \frac{D^n g}{Dx^n}$. Leibniz critical question was centred around the order n of the derivative if n does not take an integer form and instead takes a fractional form such as $n = \frac{1}{2}$. Following that question, many well[40, 53, 2, 38, 7] known mathematicians such as Euler, Liouville, Laplace, Riemann and others were attracted to this topic of interest and that went on for many years. Fractional calculus [40, 38] is considered an extension of the classical calculus and thus classified as such with one [38, 37] class representing the differential equations with integer order and the other representing the differential equations with non-integer order. Niels Henrik Abel in his work in 1823 came with a [40] generalised version of

tautochrone problem [1] that became known as Abel's mechanical problem and established that for some reasons the solution cannot be determined by applying the integral transform which can be presented as a fractional derivative

$$G = \int_0^s (s-t)^{-1/2} f(t)dt, \qquad G = const. \tag{3.2.1}$$

This solution caught [40, 29] Joseph Liouville's attention and he subsequently made a remarkable study, in the fractional calculus with major breakthrough in 1832 when he was able to demonstrate the results of his work in potential theory. It was Liouville who endeavoured to generalise the fractional derivative [40] and proposed what became known the Liouville's first formula to evaluate the derivative of order β

$$D_t^{\beta} f(t) = \sum_{i=0}^{\infty} b_i a_i^a e^{a_i t}. \tag{3.2.2}$$

This formula was found not to be a general definition of fractional derivative. In an attempt to overcome the shortcoming, he worked hard to come up with the second definition using a definite integral

$$I = \int_0^{\infty} s^{\alpha-1} e^{-ts} ds, \qquad \alpha > 0, x > 0. \tag{3.2.3}$$

Using this definition, Liouville [40, 29] derived what came to be known as the second Liouville's formula

$$D_t^{\varphi} t^{-\phi} = (-)^{\varphi} \frac{\Gamma(\varphi + \phi)}{\Gamma(\phi)} t^{-\varphi-\phi}, \qquad \phi > 0. \tag{3.2.4}$$

That attempt on the second definition by Liouville was also considered unsuitable to be a general definition of fractional derivative. It was during his student days when [40] G. F. Bernhard Riemann wrote a paper in which bold steps were made in the advancement of fractional calculus in 1853. The paper was regrettably only published after his passing on in 1892. It started when [40] Riemann looked to generalise the Taylor series and derived the definition involving integrals that are definite. This definition could be

[1] **A tautochrone** is [40] that part of the curve where the time interval for an object running down with no friction to the lowest point of the curve at constant gravity is not dependent on the object starting point.

applied to some power series involving the non integer exponents

$$D_{a,t}^{-\beta} g(t) = \frac{1}{\Gamma(\beta)} \int_a^t (t-s)^{\beta-1} g(s) ds + \xi(t) \tag{3.2.5}$$

and it has become a widely used modern definition of [6, 29, 35, 10, 16] fractional integral without the complimentary function $\xi(x)$. If the [40] expression in (3.2.5) has lower terminal $a = -\infty$ then the equation becomes what is known as the Liouville Fractional Integral and setting $a = 0$, the resulting equation is the commonly known Riemann Fractional Integral. On the other hand the expression in (3.2.5) assigned some lower value a it then becomes what is referred as Riemann-Liouville Fractional Integral defined as

$${}_\beta J_t^\beta g(t) = \frac{1}{\Gamma(\beta)} \int_a^t \frac{g(\varphi)}{(t-\varphi)^{1-\varphi}} d\varphi, \qquad (\beta \in \mathbb{R}_+) \tag{3.2.6}$$

where $a < b$ for $a, b \in \mathbb{R}$. The Riemann–Liouville fractional [39, 45, 9, 14, 27] integral in (3.2.6) converges for integrable function g with $\beta > 1$. The associated Riemann–Liouville fractional derivative of order $\beta > 0 (\beta \in \mathbb{R})$ can be defined by

$$\begin{aligned} {}^{RL} D_t^\beta g(t) =& \frac{d}{dt} J^{1-\beta} g(t), \\ =& \frac{1}{\Gamma(1-\beta)} \frac{d}{dt} \int_a^t g(\varphi)(t-\varphi)^{-\beta} d\varphi, \qquad 0 < \beta \leq 1, \qquad t > 0. \end{aligned} \tag{3.2.7}$$

It was in [40, 39, 2] 1967 when Michele Caputo after identifying some of the shortcomings in the initial conditions associated with the definition of Riemann–Liouville which made it difficult to apply it to real-life problems, reformulated the definition to use the initial conditions the same as the integer order differential equations would require them. In that way Riemann–Liouville fractional derivative[6, 40, 30, 7, 4, 24, 2] became the stepping stone for the fractional derivative proposed by Caputo and is defined by

$$\begin{aligned} {}^{C} D_t^\beta g(t) =& J^{1-\beta} \frac{d}{dt} g(t), \\ =& \frac{1}{\Gamma(1-\beta)} \int_a^t \frac{\frac{dg(\varphi)}{d\varphi}}{(t-\varphi)^\beta} d\varphi. \end{aligned} \tag{3.2.8}$$

These definitions, [10] the Riemann–Liouville and Caputo are known to be nonlocal and fractional operators. They are still useful in solving real life situations with remarkable success. However, it was found that these fractional operators have some notable benefits and drawbacks and they are outlined below.

Associated advantages for the Riemann-Liouville as well as Caputo fractional derivative

The need for an [10, 29] arbitrary function to be continuous or differentiable does not apply to the Riemann–Liouville definition. In Caputo fractional derivative[10, 29], the traditional initial conditions and boundary conditions are allowed when one is describing the problem. It is furthermore noted that the constant derivative in Caputo definition is zero.

Associated disadvantages for Riemann-Liouville as well as Caputo fractional derivative

There are [10, 29] identifiable or notable drawbacks found in Riemann–Liouville fractional derivative when modelling real world problems. Firstly, the [10, 29] constant derivative fails to become a zero. Secondly, in a situation where the original function is constant, the resulting derivative possesses a singularity that is at the origin thus reducing the areas where the Riemann–Liouville fractional derivative can be applied. In [10, 29]the case of Caputo derivative the regularity conditions for differentiability that are required are much higher. We have that the Caputo fractional derivative sense is only defined for functions that are differentiable while it is considered that functions that have no first-order could produce fractional derivatives with order smaller than one in the Riemann–Liouville fractional derivative sense.

A new Riemann–Liouville fractional derivative [28] with order β and a non-singular kernel derivative was proposed and is defined as

$$^{NRL}D_t^{\beta} f(t) = \frac{(2-\beta)M(\beta)}{2(1-\beta)} \frac{d}{dt} \int_0^t f(\varphi) exp\left[\frac{-\beta(t-\varphi)}{(1-\beta)}\right] d\varphi. \tag{3.2.9}$$

Recently, as a result [3, 29] of some complaints which were made emanating from the complications in the application of fractional differential equations, a proposition was made by Caputo and Fabrizio for a new definition that has fractional time factor derivative and has no singularity of order β and is given by

Definition 3.2.1. *Let $g \in H^1(a,b), b > a, a \in [0,1]$, we have that, the definition of the Caputo and Fabrizio fractional derivative is:*

$$^{CF}_{\beta}D_t^{\beta}(g(t)) = \frac{N(\beta)}{1-\beta} \int_b^t g'(\tau) exp\left[-\beta\frac{t-\tau}{1-\beta}\right] d\tau, \tag{3.2.10}$$

where $N(\beta)$ is a normalisation function such that $N(0) = N(1) = 1$, and it assumes two different representations of the temporal and spatial variables. Let us consider the case where [3, 29] the function does not belong to $H^1(a, b)$ then the above derivative will take the form

$$ {}^{CF}_{\beta}D^{\beta}_{t}(g(t)) = \frac{\beta N(\beta)}{1-\beta}\int_{b}^{t}(g(t)-g(\varphi))exp\bigg[-\beta\frac{t-\tau}{1-\beta}\bigg]d\tau. \tag{3.2.11} $$

Then, if $\psi = \dfrac{1-\beta}{\beta} \in [0, \infty), \beta = \dfrac{1}{1+\psi} \in [0, 1]$, then the equation assumes the form

$$ {}^{CF}_{\beta}D^{\beta}_{t}(g(t)) = \frac{M(\psi)}{\psi}\int_{b}^{t}g'(\varphi)exp\bigg[-\frac{t-\varphi}{\psi}\bigg]d\varphi, \qquad M(0) = M(\infty) = 1. $$

Even with this definition, [3, 56, 29] there were a number of issues that were pointed out in the fields of electromagnetics and thermal media to mention just a few. The issues in Caputo and Fabrizio definition include the fact that the kernel was not non-local. Another issue was [3, 56, 29] that the associated anti-derivative is regarded as the average of the function and its integral and a conclusion was made that the operator was not a fractional derivative but a filter. It remains true that [3, 56, 29] despite the shortcomings identified, much success was achieved with this definition. The Caputo and Fabrizio fractional derivative was used in the fields [56] of thermal science, engineering, groundwater studies, diffusion model and many others

3.2.2 Atangana-Baleanu derivatives with fractional order

It was Atangana and Koca in [3, 56] who pointed out that the solution of equation ${}^{CF}_{0}D^{\beta}_{t}(g(t)) = g(t)$ did not represent a special function but rather an exponential function. Atangana and Baleanu worked [3, 56, 29] to solve the issue identified against Caputo-Fabrizio by proposing a much better version of derivative with no singular kernel that became known as Atangana-Baleanu fractional derivative in Riemann-Liouville sense and Atangana-Baleanu fractional derivative in Caputo sense which is based on the popular Mittag-Leffler function and the generalised Mittag-Leffler function known to modelling complex problems. The Mittag-Leffler is regarded as the solution of the fractional differential equation

$$ \frac{d^{\eta}z}{dx^{\eta}} = \eta z, \quad 0 < \eta < 1. $$

one parameter Mittag-Leffler function

$$E_\beta(-t^\eta) = \sum_{k=1}^{\infty} \frac{(-t)^{\eta k}}{\Gamma(\eta k + 1)} \tag{3.2.12}$$

We then have the Taylor series of $exp(-(t-z))$ at t, we have

$$exp(-\eta(t-z)) = \sum_{k=0}^{\infty} \frac{(-\eta(t-z))^k}{k!}. \tag{3.2.13}$$

Setting $\eta = \dfrac{\eta}{1-\eta}$ and replace (3.2.12) into [3] Caputo and Fabrizio fractional derivative, it is then concluded that

$${}^{CF}_{\eta}D^{\eta}_{t}(g(t)) = \frac{N(\eta)}{1-\eta} \sum_{k=0}^{\infty} \frac{(-\eta)^k}{k!} \int_b^t \frac{dg(z)}{dz}(t-z)^k dz. \tag{3.2.14}$$

We replace $k!$ by $\Gamma(\eta k + 1)$ and $(t-z)^k$ by $(t-z)^{\eta k}$ in (3.2.14) to solve the issue of non-locality, and we have

$${}^{CF}_{\eta}D^{\eta}_{t}(g(t)) = \frac{N(\eta)}{1-\eta} \sum_{k=0}^{\infty} \frac{(-\eta)^k}{\Gamma(\eta k + 1)} \int_b^t \frac{dg(z)}{dz}(t-z)^{\eta k} dz. \tag{3.2.15}$$

Definition 3.2.2. *Let $g \in H^1(a,b), b > a, \eta \in [0,1]$, [3, 56, 28]then the definition of the new fractional derivative (Atangana-Baleanu fractional derivative in Riemann-Liouville sense) is given as:*

$${}^{ABR}_{\eta}D^{\eta}_{t}g(t) = \frac{M(\eta)}{(1-\eta)} \frac{d}{dt} \int_a^t g(\varphi) E_\eta \left[-\eta \frac{(t-\varphi)^\eta}{1-\eta} \right] d\varphi. \tag{3.2.16}$$

Definition 3.2.3. *Let $g \in H^1(a,b), b > a, \eta \in [0,1]$, [3, 56, 28]then the definition of the new fractional derivative (Atangana-Baleanu fractional derivative in Caputo sense) is given as:*

$${}^{ABC}_{\eta}D^{\eta}_{t}(g(t)) = \frac{M(\eta)}{(1-\eta)} \int_a^t g'(\varphi) E_\eta \left[-\eta \frac{(t-\varphi)^\eta}{1-\eta} \right] d\varphi, \tag{3.2.17}$$

In the definition 3.2.3 [3, 56] Atangana-Baleanu fractional derivative in Caputo sense, the M is said to be the same as the properties in Caputo and Fabrizio case. The definition become [3, 56] a useful tool in solving real-life phenomenon with greater advantages when using Laplace transform for solving physical problems.

Definition 3.2.4. *[3, 56, 28] The fractional integral associated to the new fractional derivative with non-local kernel (Atangana-Baleanu fractional integral) is defined as:*

$$ {}^{AB}_{\eta}J^{\eta}_{t}\big[g(t)\big] = \frac{\eta}{M(\beta)\Gamma(\eta)}g(t) + \int_{a}^{t} g(\varphi)(t-\varphi)^{\eta-1}d\varphi. \tag{3.2.18} $$

Since the Atangana-Baleanu fractional order derivative is based on the generalised Mittag-Leffler function that has non-local and non-singular kernel, provides the derivative the ability to sufficiently describe complex real life problems than the power function. The Mittag-Leffler function used as a kernel in the Atangana-Baleanu fractional order derivative, guarantees the nonsingularity. Furthermore, the [3] Atangana-Baleanu fractional order derivative better describe problems with memory effects.

3.2.3 Discussion on the fractional derivatives with two parameters having non-singular and non-local kernel

In [23], we established that, it was in fact Doungmo Goufo who raises another question regarding the influence the variable η in a double parameter Mittag-Leffler function $E_{\xi,\eta}(p)$ for $p \in \mathbb{C}$ might have on chaotic behaviour in simple non-linear system such as Lorenz. This follows after the singularity and locality issues were addressed in the Caputo and Fabrizio fractional derivative.
It is in [23] that Doungmo Goufo proposed another fractional derivative consisting of double variables or parameters, non-singular kernel and non-local kernel. This two parameter derivative is fundamentally aligned to the generalised Mittag-Leffler function introduced in 1905 by Wiman with two parameters. The function was subsequently improved by among other authors that includes Agarwal, Erdelyi, Humbert, Humbert and Agarwal and is defined as

$$ E_{\xi,\eta}(p) = \sum_{k=0}^{\infty} \frac{p^k}{\Gamma(\xi k + \eta)}, \xi, \eta, p \in \mathbb{C}, \mathcal{R}(\eta) > 0, \tag{3.2.19} $$

which generalises the associated one-parameter definition.

Definition 3.2.5 (Fractional derivative with two parameters in Caputo sense)**.** *[23] Suppose f is a function contained in $G^1(u,v); v > u; \xi \in [0;1], \eta \in (0, +\infty)$, we then have that, the fractional derivative with two parameters of order ξ in Caputo sense given*

η is defined as

$$ {}_{a}^{gc}D_{t}^{\xi,\eta}f(t) = \frac{\eta M(\xi,\eta)}{(\eta-\xi)}\int_{a}^{t}\dot{f}(\varphi)(t-\varphi)^{\eta-1}E_{\xi,\eta}\left[-\frac{\xi\eta(t-\varphi)^{\xi}}{\eta-\xi}\right]d\varphi \tag{3.2.20} $$

where $M(\xi,\eta)$ represents the normalization function with two parameters such that $M(0,1) = M(1,1) = 1$.

The parameter η becomes zero for a 2-GC derivative of any order ξ where the function $f(t)$ is constant. At $t = \varphi$, the kernel has no singularity. In addition, it is as a results of [23] the two-parameter Mittag-Leffler function $E_{\xi,\eta}\left[-\frac{\xi\eta(t-\varphi)^{\xi}}{\eta-\xi}\right]$, that the kernel becomes non-local. Let us consider the function f such that $f \notin G^1(a,b)$, then it follows that for any function $f \in S^1(-\infty,b)$, then the 2-GC derivative of order ξ with η known is given as [23]

$$ {}_{a}^{gc}D_{t}^{\xi,\eta}f(t) = \frac{\xi M(\xi,\eta)}{(\eta-\xi)}\int_{-\infty}^{t}(f(t)-f(\varphi))(t-\varphi)^{\eta-1}\times E_{\xi,\eta}\left[-\frac{\xi\eta(t-\varphi)^{\xi}}{\eta-\xi}\right]d\varphi. \tag{3.2.21} $$

The equation (3.2.20) can [23] also be written as

$$ {}_{a}^{gc}D_{t}^{\xi,\eta}f(t) = \frac{\eta M(\xi,\eta)}{(\eta-\xi)}(\dot{f} * v(t)), \tag{3.2.22} $$

where

$$ v(t) = t^{\eta-1}E_{\xi,\eta}\left[-\frac{\xi\eta t^{\xi}}{\eta-\xi}\right], \tag{3.2.23} $$

and the * in (3.2.22) [23] representing the Laplace convolution operator. The convolution integral function possesses properties that are useful in filtering and image processing and is given as

$$ f(t) * v(t) = \int_{a}^{t} f(\varphi)v(t-\varphi)d\varphi. $$

Definition 3.2.6. *(Fractional derivative with Two parameters in Riemann-Liouville sense)[23] Suppose f is a function contained in $G^1(u,v); v > u; \xi \in [0;1], \eta \in (0,+\infty)$, we then have that, the fractional derivative with two parameters of order ξ in Riemann-Liouville-sense given η (or this is otherwise called the 2-GRL [Goufo-Riemann- Liouville] derivative of order ξ given η) is defined as*

$$ {}_{a}^{gc}D_{t}^{\xi,\eta}f(t) = \frac{\eta M(\xi,\eta)}{(\eta-\xi)}\int_{a}^{t}f(\varphi)(t-\varphi)^{\eta-1}E_{\xi,\eta}\left[-\frac{\xi\eta(t-\varphi)^{\xi}}{\eta-\xi}\right]d\varphi \tag{3.2.24} $$

with the unknowns retaining the definitions similar to (3.2.20)
and therefore, the equation can be represented as

$$ {}_{a}^{gc}D_{t}^{\xi,\eta}f(t) = \frac{\eta M(\xi,\eta)}{(\eta-\xi)}(f(t) * v(t)), \tag{3.2.25} $$

and the term $v(t)$ is as expressed as in (3.2.23).

The two definitions (3.2.5) and (3.2.6) are verified [23] in order to determine whether the fractional derivative with non-singular and non-local kernel for a single parameter in (3.2.3) and (3.2.2) could be recovered:

Special case: For the fractional derivative given the order ξ and $\eta = 1$

Taking a case where $\eta = 1$, then [23] the non-local kernel $E_{\xi,\eta}\left[-\frac{\xi\eta(t-\varphi)^{\xi}}{\eta-\xi}\right]$, becomes

$$ E_{\xi,1}\left[-\frac{\xi(t-\varphi)^{\xi}}{1-\xi}\right] = E_{\xi}\left[-\frac{\xi(t-\varphi)^{\xi}}{1-\xi}\right], $$

and (3.2.20) become

$$ {}_{a}^{gc}D_{t}^{\xi,1}f(t) = \frac{\tilde{M}(\xi)}{(1-\xi)}\int_{a}^{t}\dot{f}(\varphi)E_{\xi}\left[-\frac{\xi(t-\varphi)^{\xi}}{1-\xi}\right]d\varphi = {}_{a}^{ABC}D_{t}^{\xi}f(t), \tag{3.2.26} $$

where $\tilde{M}(\xi) = M(\xi,1)$ represents the [23] normalisation function in Caputo and Fabrizio fractional derivative. The single parameter fractional derivative with non-local and non-singular kernel in Caputo sense ${}_{a}^{ABC}D_{t}^{\xi}f(t)$ proposed by Atangana and Baleanu has been recovered and hence the 2-GC derivative of order ξ knowing $\eta = 1$ satisfies the properties of ${}_{a}^{ABC}D_{t}^{\xi}f(t)$. It is also shown that [23]

$$ \lim_{\xi\to 1}{}_{a}^{gc}D_{t}^{\xi,1}f(t) = \lim_{\rho\to 0}\frac{W(\rho)}{(\rho)}\int_{a}^{t}\dot{f}(\varphi)exp\left[-\frac{\xi(t-\varphi)}{\rho}\right]d\varphi = \dot{f}(t), \tag{3.2.27} $$

and

$$ \lim_{\xi\to 0}{}_{a}^{gc}D_{t}^{\xi,1}f(t) = \lim_{\rho\to +\infty}\frac{W(\rho)}{(\rho)}\int_{a}^{t}\dot{f}(\varphi)exp\left[-\frac{\xi(t-\varphi)}{\rho}\right]d\varphi = f(t)-f(a), \tag{3.2.28} $$

where $\rho = \frac{1-\xi}{\xi} \in [0, +\infty]$ in all cases where $\xi = \frac{1}{1+\rho} \in [0, 1]$ and $W(\rho)$ becomes [23] the corresponding normalisation term of $\tilde{M}(\xi)$ with $W(0) = W(\infty) = 1$.
For the [23] compatibility relations of the fractional derivative in Caputo-sense double variables, we have that

$$ {}^{gc}_{a}D^{1,1}_{t} f(t) \sim \frac{df(t)}{dt} \tag{3.2.29} $$

and if $f(a) = 0$, then

$$ {}^{gc}_{a}D^{0,1}_{t} f(t) \sim f(t). \tag{3.2.30} $$

similarly (3.2.24) becomes

$$ {}^{gr}_{a}D^{\xi,1}_{t} f(t) = \frac{\tilde{M}(\xi)}{(1-\xi)} \frac{d}{dt} \int_a^t f(\varphi) E_z \left[-\frac{\xi(t-\varphi)^{\xi}}{1-\xi} \right] d\varphi = {}^{ABC}_{a}D^{\xi}_{t} f(t). \tag{3.2.31} $$

The [23] fractional derivative with non-local and non-singular kernel in Riemann-Liouville sense ${}^{ABC}_{a}D^{\xi}_{t} f(t)$ has been recovered. This makes the 2-GRL derivative of order ξ when $\eta = 1$ is known to also satisfy the properties of ${}^{ABC}_{a}D^{\xi}_{t} f(t)$. It is also shown that [23]

$$ \lim_{\xi \to 1} {}^{gr}_{a}D^{\xi,1}_{t} f(t) = \lim_{\rho \to 0} \frac{W(\rho)}{(\rho)} \frac{d}{dt} \int_a^t f(\varphi) exp \left[-\frac{\xi(t-\varphi)}{\rho} \right] d\varphi = \dot{f}(t), \tag{3.2.32} $$

and

$$ \lim_{\xi \to 0} {}^{gr}_{a}D^{\xi,1}_{t} f(t) = \lim_{\rho \to +\infty} \frac{W(\rho)}{(\rho)} \frac{d}{dt} \int_a^t f(\varphi) exp \left[-\frac{\xi(t-\varphi)}{\rho} \right] d\varphi = f(t). \tag{3.2.33} $$

To continue[23] obtaining the compatibility for the fractional derivative in Riemann-Liouville sense of double variables, we proceed as follows

$$ {}^{gr}_{a}D^{1,1}_{t} f(t) \sim \frac{df(t)}{dt}, \tag{3.2.34} $$

and if $f(a) = 0$, then

$$ {}^{gr}_{a}D^{0,1}_{t} f(t) \sim f(t). \tag{3.2.35} $$

The following is the fractional integral [23] related to the derivatives ${}^{gc}_{a}D^{\xi,1}$ and ${}^{gr}_{a}D^{\xi,1}$ and can be defined as

$$ J^{\xi,1}_{t} f(t) = \frac{1-\xi}{W(\xi)} f(t) + \frac{\xi}{\Gamma(\xi) W(\xi)} \int_0^t f(t)(t-\varphi)^{\xi-1} d\varphi. \tag{3.2.36} $$

3.3 Description of the model

The 3D Lorenz system [59] defined by

$$\begin{aligned} {}^{ABC}D_t^{\phi}x(t) &= -\xi(-x+y),\\ {}^{ABC}D_t^{\phi}y(t) &= \Phi x - y - xz,\\ {}^{ABC}D_t^{\phi}z(t) &= -\gamma z + xy \end{aligned} \tag{3.3.1}$$

where x, y, and z are state variables and ξ, Φ and γ are positive parameters. The proposed four-dimensional hyperchaotic system was developed from the Lorenz three-dimensional model by adding a state variable w in (3.3.1) to the second differential equation and $0.67w$ to the third equation and is defined as

$$\begin{aligned} {}^{ABC}D_t^{\phi}x(t) &= -\xi(-x+y),\\ {}^{ABC}D_t^{\phi}y(t) &= \Phi x - y - xz,\\ {}^{ABC}D_t^{\phi}z(t) &= -\gamma z + 0.67w + xy,\\ {}^{ABC}D_t^{\phi}w(t) &= \psi w - xz \end{aligned} \tag{3.3.2}$$

where x, y, z and w are state variables and ξ, Φ, γ and ψ are nonnegative parameters.

The four-dimensional system (3.3.2), [28, 39] allows us to determine the non-positive convergence $Div = -\xi$, and thus indicating that the model is actually dissipative. As time becomes larger the model then becomes chaotic, resulting into attractors. Part of what we need to achieve in the analysis of the hyperchaotic system, is to determine the system equilibrium points necessary to understand the complex dynamics of the system. To achieve that, we set

$$\begin{cases} 0 = {}^{ABC}D_t^{\phi}x(t) = -\xi(-x+y),\\ 0 = {}^{ABC}D_t^{\phi}y(t) = \Phi x - y - xz,\\ 0 = {}^{ABC}D_t^{\phi}z(t) = -\gamma z + 0.67w + xy,\\ 0 = {}^{ABC}D_t^{\phi}w(t) = \psi w - xz \end{cases} \tag{3.3.3}$$

giving the two solutions points $[\nmid \Phi^{0.5}, \nmid \Phi^{0.5}, 0.0]$. The [28, 1] stability of the equilibrium points is determined by using the stability criteria for fractional model. These are actually the unstable equilibrium points for the system (3.3.3). Linearizing the system (3.3.3) at these points $[\nmid \Phi^{0.5}, \nmid \Phi^{0.5}, 0.0]$, allows us to find the eigenvalues λ_e which

satisfies the constraint

$$\phi\frac{\pi}{2} < [arg\lambda_e]. \tag{3.3.4}$$

We apply (3.3.3) the initial conditions as stated below, to further solve the system:

$$\left.\begin{aligned} x(0) &= s(x),\\ y(0) &= h(y),\\ z(0) &= m(z,),\\ w(0) &= l(w) \end{aligned}\right\}. \tag{3.3.5}$$

Now, here we use [28] the anti-derivative in (3.1.2) which then gives the system

$$\begin{cases} x(t) - s = {}^{AB}\mathbf{J}_t^{\phi}[-\xi(-x+y)],\\ y(t) - h = {}^{AB}\mathbf{J}_t^{\phi}[\Phi x - y - xz],\\ z(t) - m = {}^{AB}\mathbf{J}_t^{\phi}[-\gamma z + 0.67w + xy],\\ w(t) - l = {}^{AB}\mathbf{J}_t^{\phi}[\psi w - xz] \end{cases} \tag{3.3.6}$$

or equivalently, we have

$$\begin{cases} x(t) - s = \dfrac{\phi}{\mathbf{W}(\phi)\Gamma(\phi)}\displaystyle\int_0^t (t-\varphi)^{\phi-1}\{-\xi[-x(\varphi)+y(\varphi)]\}d\varphi + \dfrac{1-\phi}{\mathbf{W}(\phi)}\{-\xi[-x(t)+y(t)]\},\\ y(t) - h = \dfrac{\phi}{\mathbf{W}(\phi)\Gamma(\phi)}\displaystyle\int_0^t (t-\varphi)^{\phi-1}[\Phi x(\varphi) - y(\varphi) - x(\varphi)z(\varphi)]d\varphi + \dfrac{1-\phi}{\mathbf{W}(\phi)}[\Phi x(t) - y(t) - x(t)z(t)],\\ z(t) - m = \dfrac{\phi}{\mathbf{W}(\phi)\Gamma(\phi)}\displaystyle\int_0^t (t-\varphi)^{\phi-1}[-\gamma z(\varphi) + 0.67w(\varphi) + x(\varphi)y(\varphi)]d\varphi + \dfrac{1-\phi}{\mathbf{W}(\phi)}[-\gamma z(t)\\ \qquad\qquad + 0.67w(t) + x(t)y(t)],\\ w(t) - l = \dfrac{\phi}{\mathbf{W}(\phi)\Gamma(\phi)}\displaystyle\int_0^t (t-\varphi)^{\phi-1}[\psi w(\varphi) - x(\varphi)z(\varphi)]d\varphi + \dfrac{1-\phi}{\mathbf{W}(\phi)}[\psi w(t) - x(t)z(t)] \end{cases} \tag{3.3.7}$$

Now, the necessary state vectors are defined as

$$\mathbf{p}(t) = \begin{pmatrix} x(t)\\ y(t)\\ z(t)\\ w(t) \end{pmatrix}.$$

and that

$$\mathbf{p}_0(x,y,z) = \mathbf{p}(0) = \begin{pmatrix} u \\ v \\ m \\ l \end{pmatrix}$$

for some matrix defined as

$$\mathcal{M}[\mathbf{p}(t),t] = \begin{pmatrix} \mathcal{M}_1[\mathbf{p}(t),t] \\ \mathcal{M}_2[\mathbf{p}(t),t] \\ \mathcal{M}_3[\mathbf{p}(t),t] \\ \mathcal{M}_4[\mathbf{p}(t),t] \end{pmatrix},$$

where

$$\begin{cases} \mathcal{M}_1[\mathbf{p}(t),t] = [-\xi(-x+y)], \\ \mathcal{M}_2[\mathbf{p}(t),t] = [\Phi x - y - xz], \\ \mathcal{M}_3[\mathbf{p}(t),t] = [-\gamma z + 0.67w + xy], \\ \mathcal{M}_4[\mathbf{p}(t),t] = [\psi w - xz] \end{cases} \tag{3.3.8}$$

The operator $\mathcal{M}$ satisfies the Lipschitz [28] condition with respect to the state variable $\mathbf{p}$, and thus a real number $e_1 \geq 0$ exists such that the relation

$$\| \mathcal{M}(\mathbf{p},t) - \mathcal{M}(\bar{\mathbf{p}},t) \| \leq e_1 \| \mathbf{p} - \bar{\mathbf{p}} \| \tag{3.3.9}$$

holds, with $\mathbf{p}$ and $\bar{\mathbf{p}}$ representing the arbitrary system states. Furthermore, we have the norm $\| \cdot \| = \| \cdot \|_{\mathfrak{R}\ (3,1)}$ defined [28] as the sum total derived from $\mathfrak{R}_{\ 3,1}$. Representing some 3×1 real matrices

$$\| \mathbf{p} \| = {}_{1 \leq j \leq 3}^{max} = \| \mathbf{p}_j \|_{H^1},$$

and here $\| \mathbf{p}_j \|_{G^1}$ [28, 58] represents the norm within the space $G^1(0;p), p$ greater than zero and is given by

$$\| \mathbf{p}(t) \|_{H^1}^2 = \| \mathbf{p}(t) \|_{T^2}^2 + \| \mathbf{p}'(t) \|_{T^2}^2 .$$

From the above, we are able to derive the following system of iterations

$$\begin{cases} x_0 = x(0) = s, \\ y_0 = y(0) = h, \\ z_0 = z(0) = l, \\ w_0 = w(0) = m \end{cases} \tag{3.3.10}$$

and

$$\begin{cases} x_{n+1}(t)-s = \dfrac{\phi}{\mathbf{W}(\phi)\Gamma(\phi)}\displaystyle\int_0^t (t-\varphi)^{\phi-1}\{-\xi[-x_n(\varphi)+y_n(\varphi)]\}d\varphi + \dfrac{1-\phi}{\mathbf{W}(\phi)}\{-\xi[-x_n(t)+y_n(t)]\}, \\ y_{n+1}(t)-h = \dfrac{\phi}{\mathbf{W}(\phi)\Gamma(\phi)}\displaystyle\int_0^t (t-\varphi)^{\phi-1}[\Phi x_n(\varphi)-y_n(\varphi)-x_n(\varphi)z_n(\varphi)]d\varphi \\ \qquad + \dfrac{1-\phi}{\mathbf{W}(\phi)}[\Phi x_n(\varphi)-y_n(t)-x_n(\varphi)z_n(t)], \\ z_{n+1}(t)-m = \dfrac{\phi}{\mathbf{W}(\phi)\Gamma(\phi)}\displaystyle\int_0^t (t-\varphi)^{\phi-1}[-\gamma z_n(\varphi)+0.67w_n(\varphi)+x_n(\varphi)y_n(\varphi)]d\varphi + \\ \qquad \dfrac{1-\phi}{\mathbf{W}(\phi)}[-\gamma z_n(t)+0.67w_n(t)+x_n(t)y_n(t)], \\ w_{n+1}(t)-l = \dfrac{\phi}{\mathbf{W}(\phi)\Gamma(\phi)}\displaystyle\int_0^t (t-\varphi)^{\phi-1}[\psi w(\varphi)-x_n(\varphi)z_n(\varphi)]d\varphi + \dfrac{1-\phi}{\mathbf{W}(\phi)}[\psi w_n(t)-x_n(t)z_n(t)] \end{cases} \tag{3.3.11}$$

for $n \in W$. The unique solution of the form below is finally achieved and is defined as

$$\mathbf{p}(t) = \begin{pmatrix} x(t) \\ y(t) \\ z(t) \\ w(t) \end{pmatrix} = \lim_{n\to\infty} \mathbf{p}_n(t) = \begin{pmatrix} x_n(t) \\ y_n(t) \\ z_n(t) \\ w_n(t) \end{pmatrix}.$$

The proof at this point is still incomplete until [28] the operator contractiveness with respect to $\mathbf{p}$ is established:

$$\xi\mathbf{p}(t) = \mathbf{p}_0 + \frac{\phi}{\mathbf{W}(\phi)\Gamma(\phi)}\int_0^t (t-\varphi)^{\phi-1} W[\mathbf{p}(\varphi),\varphi]d\varphi + \frac{1-\phi}{\mathbf{W}(\phi)}\mathcal{M}[\mathbf{p}(t),t]. \tag{3.3.12}$$

Using (3.3.9), we now consider the states $\mathbf{p}$ and $\bar{\mathbf{p}}$, and using the Lipschitz continuity to find the Lipschitz constant, we have

$$\begin{aligned} \|\xi\mathbf{p}(t)-\xi\bar{\mathbf{p}}(t)\| &= \|\frac{\phi}{\mathbf{W}(\phi)\Gamma(\phi)}\int_0^t (t-\varphi)^{\phi-1} W[\mathbf{p}(\varphi),\varphi]-W[\bar{\mathbf{p}}(\varphi),\varphi]d\varphi + \frac{1-\phi}{\mathbf{W}(\phi)}\mathcal{M}[\mathbf{p}(t),t]-\mathcal{M}[\bar{\mathbf{p}}(\mathbf{t}),t]\| \\ &\le \frac{\phi}{\mathbf{W}(\phi)\Gamma(\phi)}\int_0^t (t-\varphi)^{\phi-1}\|W[\mathbf{p}(\varphi),\varphi]-W[\bar{\mathbf{p}}(\varphi),\varphi]\|d\varphi + \frac{1-\phi}{\mathbf{W}(\phi)}\|\mathcal{M}[\mathbf{p}(t),t]-\mathcal{M}[\bar{\mathbf{p}}(\mathbf{t}),t]\| \\ &\le \frac{\phi}{\mathbf{W}(\phi)\Gamma(\phi)}\int_0^t (t-\varphi)^{\phi-1} e_1 \parallel \mathbf{p}(\varphi)-\bar{\mathbf{p}}(\varphi)\parallel d\varphi + \frac{1-\phi}{\mathbf{W}(\phi)} e_1 \parallel \mathbf{p}(t)-\bar{\mathbf{p}}(\mathbf{t})\parallel. \end{aligned} \tag{3.3.13}$$

Integrating for $t \in (0,p), p>0$, we have

$$\parallel \xi\mathbf{p}(t)-\xi\bar{\mathbf{p}}(t)\parallel \le \mathbf{w}(\phi)\parallel \mathbf{p}(t)-\bar{\mathbf{p}}(\mathbf{t})\parallel. \tag{3.3.14}$$

The coefficient $\mathbf{w}(\phi)$ in (3.3.14) is the Lipschitz constant and is expressed as

$$\mathbf{w}(\phi) = \frac{e_1 p^{\phi}}{\phi \mathbf{W}(\phi)\Gamma(\phi)} - \frac{\phi e_1}{\mathbf{W}(\phi)}.$$

Chapter 4

Laplace Adams-Bashforth Method:with Error Analysis and Convergence

4.1 Introduction

A method that [22] generalises how the Adams-Bashforth is used to solve or treat Partial Differential Equations with nonlocal and local operators is presented. Here, the two-step Adams-Bashforth numerical scheme is derived in Laplace space and the resulting solution is taken back into real space through the use of inverse Laplace transform. The Adam-Bashforth [22, 32] numerical method was extended to solve partial differential equations due to its efficiency and accuracy. That is achieved by elimination of one variable and transform the partial differential equation to the ordinary differential equation using the Laplace transform. This powerful numerical algorithm is then used to solve the fractional order derivatives.

4.2 Analysis of numerical method for partial differential equations with Integer Order

Firstly, we consider the general P.D.E [22]

$$\frac{\partial v(u,r)}{\partial r} = Mv(u,r) + Uv(u,r) \tag{4.2.1}$$

where M and U are operators of linear and non linear type respectively. Applying [22, 60] on both sides of the equation (4.2.1) the Laplace Transform for the variable u, we have

$$\begin{aligned}\mathscr{L}\left(\frac{\partial v(u,r)}{\partial r}\right) =&\mathscr{L}\Big(Mv(u,r)+Uv(u,r)\Big) \Longrightarrow\\ \frac{d}{dr}(v(s,r)) =&\mathscr{L}\Big(Mv(u,r)+Uv(u,r)\Big)\\ \frac{d}{dr}(v(r)) =&G(v,r)\end{aligned} \tag{4.2.2}$$

with $v(r) = v(s,r)$ and $G(v,r) = \mathscr{L}\Big(Mv(u,r)+Uv(u,r)\Big)$. Applying on equation (4.2.2) [22, 50, 49, 13] the Fundamental Theorem of Calculus one obtains

$$v(r) = v(r_0) + \int_0^r G(v,\rho)d\rho$$

this can also be represented by

$$v(r) = v_0 + \int_0^r G(v,\rho)d\rho$$

setting $r = r_{m+1}$, we have

$$v_{m+1} = v(r_{m+1}) = v_0 + \int_0^{r_{m+1}} G(v,\rho)d\rho$$

also, setting $r = r_m$, gives

$$v_m = v(r_m) = v_0 + \int_0^{r_m} G(v,\rho)d\rho$$

from the above it then follows that

$$\begin{aligned}v_{m+1} - v_m =& \int_0^{r_{m+1}} G(v,\rho)d\rho - \int_0^{r_n} G(v,\rho)d\rho\\ v_{m+1} - v_m =& \int_{r_m}^{r_{m+1}} G(v,\rho)d\rho\end{aligned}$$

Approximating [22, 33] $G(v,r)$ using the Lagrangian polynomial, we have

$$\begin{aligned}L(r) \approx G(v,r) =& \frac{r-r_{m-1}}{r_m - r_{m-1}}G(v,r_m) + \frac{r-r_m}{r_{m-1}-r_m}G(v,r_{m-1})\\ L(r) =& \frac{r-r_{m-1}}{r_m - r_{m-1}}G_n + \frac{r-r_m}{r_{m-1}-r_m}G_{m-1}\end{aligned}$$

therefore, the equation above is represented by

$$\begin{aligned}
v_{m+1} - v_m =& \int_{r_m}^{r_{m-1}} G(v,\rho)d\rho \\
v_{m+1} - v_m =& \int_{r_m}^{r_{m+1}} \left(\frac{r - r_{m-1}}{r_m - r_{m-1}}G_n + \frac{r - r_m}{r_{m-1} - r_m}G_{m-1}\right)dr \\
v_{m+1} - v_m =& \frac{G_m}{r_m - r_{m-1}}\int_{r_m}^{r_{m+1}}(r - r_{m-1})dr + \frac{G_{m-1}}{r_{m-1} - r_m}\int_{r_m}^{r_{m+1}}(r - r_m)dr \\
v_{m+1} - v_m =& \frac{G_m}{r_m - r_{m-1}}\left[\frac{1}{2}r^2 - rr_{m-1}\right]_{r_m}^{r_{m+1}} + \frac{G_{m-1}}{r_{m-1} - r_m}\left[\frac{1}{2}r^2 - rr_m\right]_{r_m}^{r_{m+1}}
\end{aligned}$$

We let

$$k = r_m - r_{m-1}$$

and we then have

$$\begin{aligned}
v_{m+1} - v_m =& \frac{G_m}{k}\left(\frac{1}{2}r_{m+1}^2 - r_{m+1}r_{m-1} - \frac{1}{2}r_m^2 + r_m r_{m-1}\right) - \frac{G_{m-1}}{k}\left(\frac{1}{2}r_{m+1}^2 - r_m r_{m+1} - \frac{1}{2}r_m^2 + r_m^2\right) \\
v_{m+1} - v_m =& \frac{G_m}{k}\left(\frac{1}{2}(r_{m+1} - r_m)(r_{m+1} + r_m) - r_{m-1}(r_{m+1} + r_m)\right) \\
& - \frac{G_{m-1}}{k}\left(\frac{1}{2}(r_{m+1} - r_m)(r_{m+1} + r_m) - r_m(r_{m+1} - r_m)\right) \\
v_{m+1} - v_m =& \frac{G_m}{k}\left(\frac{1}{2}k(r_{m+1} + r_m) - kr_{m-1}\right) - \frac{G_{m-1}}{k}\left(\frac{1}{2}k(r_{m+1} + r_m) - kr_m\right) \\
v_{m+1} - v_m =& G_m\left(\frac{1}{2}(r_{m+1} + r_m) - r_{m-1}\right) - G_{m-1}\left(\frac{1}{2}(r_{m+1} + r_m) - r_m\right) \\
v_{m+1} - v_m =& G_m\left(\frac{1}{2}\left((m+1)k + mk\right) - (m-1)k\right) - G_{m-1}\left(\frac{1}{2}\left((m+1)k + mk\right) - mk\right) \\
v_{m+1} - v_m =& G_n\left(mk + \frac{1}{2}k - mk + k\right) - G_{m-1}\left(mk + \frac{1}{2}k - mk\right) \\
v_{m+1} =& v_m + k\left(\frac{3}{2}G_m - \frac{1}{2}G_{m-1}\right)
\end{aligned} \tag{4.2.3}$$

In order to return into the real space, We [22, 60] apply the inverse form of Laplace transform, and this gives:

$$\begin{aligned}
\mathscr{L}^{-1}(v_{m+1}) =& \mathscr{L}^{-1}\left[v_m + k\left(\frac{3}{2}G_m - \frac{1}{2}G_{m-1}\right)\right] \\
v(u,r) =& \mathscr{L}^{-1}\left[v_m + k\left(\frac{3}{2}G_m - \frac{1}{2}G_{m-1}\right)\right]
\end{aligned}$$

4.3 The new Numerical Method for P.D.E with non integer order

The numerical scheme is illustrated by using the following general fractional P.D.E

$$\frac{\partial^{\varphi} v(u,r)}{\partial r^{\varphi}} = Mv(u,r) + Uv(u,r) \tag{4.3.1}$$

for M and U are operators of linear and non linear type respectively. We now apply [22, 60] on both sides of equation (4.3.1) the Laplace transform, and it gives

$$\mathscr{L}\left(\frac{\partial^{\varphi} v(u,r)}{\partial r^{\varphi}}\right) = \mathscr{L}\Big(Mv(u,r) + Uv(u,r)\Big)$$

By considering the fractional partial derivative in Caputo sense, the equation is

$$\begin{aligned} {}^{C}_{\varphi}D^{\varphi}_{r} v(s,r) =& \mathscr{L}\Big(Mv(u,r) + Uv(u,r)\Big) \\ {}^{C}_{\varphi}D^{\varphi}_{r} v(s,r) =& G(v,r) \end{aligned}$$

which then becomes

$${}^{C}_{\varphi}D^{\varphi}_{r} v(r) = G(v,r) \tag{4.3.2}$$

where $v(r) = v(s,r)$ and $G(v,r) = \mathscr{L}\Big(Mv(u,r) + Uv(u,r)\Big)$.
Next, the [22] fractional integral operator in Caputo sense is applied on equation (4.3.2) which gives

$$v(r) - v(r_0) = \frac{1}{\Gamma(\varphi)} \int_0^r (r-\rho)^{\varphi-1} G(v,\rho) d\rho$$

Setting $r = r_{m+1}$

$$v_{m+1=} v(r_{m+1}) = v_0 + \frac{1}{\Gamma(\varphi)} \int_0^{r_{m+1}} (r_{m+1}-\rho)^{\varphi-1} G(v,\rho) d\rho$$

Setting $r = r_n$

$$\begin{aligned} v_m =& v(r_m) = v_0 + \frac{1}{\Gamma(\varphi)} \int_0^{r_m} (r_m - \rho)^{\varphi-1} G(v,\rho) d\rho \\ v_{m+1} - v_m =& \frac{1}{\Gamma(\varphi)} \left[\int_0^{r_{m+1}} (r_{m+1} - \rho)^{\varphi-1} G(v,\rho) d\rho - \int_0^{r_m} (r_m - \rho)^{\varphi-1} G(v,\rho) d\rho \right] \\ & \int_0^{r_{m+1}} (r_{m+1} - \rho)^{\varphi-1} G(v,\rho) d\rho = \sum_{i=0}^{m} \int_{r_i}^{r_{i+1}} (r_{m+1} - \rho)^{\varphi-1} G(v,\rho) d\rho \end{aligned} \tag{4.3.3}$$

Approximating [22] $G(u,t)$ using the Lagrange polynomial, we have

$$\begin{aligned} L(r) \approx G(v,t) =& \frac{r - r_{m-1}}{r_m - r_{m-1}} G(v, r_m) + \frac{r - r_m}{r_{m-1} - r_m} G(v, r_{m-1}) \\ L(r) =& \frac{r - r_{m-1}}{r_m - r_{m-1}} G_m + \frac{r - r_m}{r_{m-1} - r_m} G_{m-1} \end{aligned}$$

The [22] fractional integral $\int_0^{r_{m+1}} (r_{m+1} - \rho)^{\varphi-1} G(v,\rho) d\rho$ in equation (4.3.3) can be expressed as

$$\begin{aligned} & \int_0^{r_{m+1}} (r_{m+1} - \rho)^{\varphi-1} G(v,\rho) d\rho = \sum_{i=0}^{m} \int_{r_i}^{r_{i+1}} (r_{m+1} - r)^{\varphi-1} \left(\frac{r - r_{m-1}}{r_m - r_{m-1}} G_m + \frac{r - r_m}{r_{m-1} - r_m} G_{m-1} \right) dr \\ &= \sum_{i=0}^{m} \left[\frac{G_m}{r_m - r_{m-1}} \int_{r_i}^{r_{i+1}} (r_{m+1} - r)^{\varphi-1} (r - r_{m-1}) dr + \frac{G_{m-1}}{r_{m-1} - r_m} \int_{r_i}^{r_{i+1}} (r_{m+1} - r)^{\varphi-1} (r - r_m) dr \right] \\ &= \sum_{i=0}^{m} \left[\frac{G_m}{k} \int_{r_i}^{r_{i+1}} (r_{m+1} - r)^{\varphi-1} (r - r_{m-1}) dr + \frac{G_{m-1}}{k} \int_{r_i}^{r_{i+1}} (r_{m+1} - r)^{\varphi-1} (r - r_m) dr \right] \end{aligned}$$

By changing the [22] variables, we let $z = r_{m+1} - r, dr = -dz, r = r_{m+1} - z$.

$$\begin{aligned} \int_{r_i}^{r_{i+1}} (r_{m+1} - r)^{\varphi-1} (r - r_{m-1}) dr =& \int_{r_{m+1}-r_i}^{r_{m+1}-r_{i+1}} z^{\varphi-1} (-z + r_{m+1} - r_{m-1}) dz \\ =& \int_{r_{m+1}-r_i}^{r_{m+1}-r_{i+1}} (z^{\varphi} - 2k z^{\varphi-1}) dz \\ =& \frac{1}{\varphi+1} \left[z^{\varphi+1} \right]_{r_{m+1}-r_j}^{r_{m+1}-r_{i+1}} - \frac{2k}{\varphi} \left[z^{\varphi} \right]_{r_{m+1}-r_j}^{r_{m+1}-r_{i+1}} \\ =& \frac{1}{\varphi+1} \left((r_{m+1} - r_{i+1})^{\varphi+1} - (r_{m+1} - r_i)^{\varphi+1} \right) \\ & - \frac{2k}{\varphi} \left((r_{m+1} - r_{i+1})^{\varphi} - (r_{m+1} - r_i)^{\varphi} \right) \end{aligned}$$

We also have

$$\begin{aligned}\int_{r_i}^{r_{i+1}}(r_{m+1}-r)^{\varphi-1}(r-r_m)dr &= -\int_{r_{m+1}-r_i}^{r_{m+1}-r_{i+1}} z^{\varphi-1}(-z+r_{m+1}-r_m)dz\\ &=\int_{r_{m+1}-r_i}^{r_{m+1}-r_{i+1}}(z^{\varphi}-kz^{\varphi-1})dz\\ &=\frac{1}{\varphi+1}\Big[z^{\varphi+1}\Big]_{r_{m+1}-r_j}^{r_{m+1-r_{i+1}}}-\frac{k}{\varphi}\Big[z^{\varphi}\Big]_{r_{m+1}-r_j}^{r_{m+1-r_{i+1}}}\\ &=\frac{1}{\varphi+1}\Big((r_{m+1}-r_{i+1})^{\varphi+1}-(r_{m+1}-r_i)^{\varphi+1}\Big)\\ &-\frac{k}{\varphi}\Big((r_{m+1}-r_{i+1})^{\varphi}-(r_{m+1}-r_i)^{\varphi}\Big)\end{aligned}$$

Which then follows that

$$\begin{aligned}&\int_0^{r_{m+1}}(r_{m+1}-\rho)^{\varphi-1}G(v,\rho)d\rho\\ &=\frac{G_m}{k}\Big\{\sum_{i=0}^{n}\Big[\frac{1}{\varphi+1}\Big((r_{m+1}-r_{i+1})^{\varphi+1}-(r_{m+1}-r_i)^{\varphi+1}\Big)\Big]\\ &-\frac{2k}{\varphi}\sum_{i=0}^{m}\Big[\Big((r_{m+1}-r_{i+1})^{\varphi}-(r_{m+1}-r_i)^{\varphi}\Big)\Big]\Big\}\\ &-\frac{G_{m-1}}{k}\Big\{\sum_{i=0}^{m}\Big[\frac{1}{\varphi+1}\Big((r_{m+1}-r_{i+1})^{\varphi+1}-(r_{m+1}-r_i)^{\varphi+1}\Big)\Big]\\ &-\frac{k}{\varphi}\sum_{i=0}^{m}\Big[\Big((r_{m+1}-r_{i+1})^{\varphi}-(r_{m+1}-r_i)^{\varphi}\Big)\Big]\Big\}\\ &=\frac{G_n}{k}\Big(\frac{1}{\varphi+1}(-(r_{m+1}-r_0)^{\varphi+1})-\frac{2k}{\varphi}(-(r_{m+1}-r_0)^{\varphi})\Big)\\ &-\frac{G_{m-1}}{k}\Big(\frac{1}{\varphi+1}(-(r_{m+1}-r_0)^{\varphi+1})-\frac{k}{\varphi}(-(r_{m+1}-r_0)^{\varphi})\Big)\\ &=\frac{G_m}{k}\Big(\frac{-(m+1)^{\varphi+1}k^{\varphi+1}}{\varphi+1}+\frac{2k(m+1)^{\varphi}k^{\varphi}}{\varphi}\Big)\\ &-\frac{G_{m-1}}{k}\Big(\frac{-(m+1)^{\varphi+1}k^{\varphi+1}}{\varphi+1}+\frac{k(n+1)^{\varphi}k^{\varphi}}{\varphi}\Big)\\ &=k^{\varphi}\Big[\Big(\frac{2(m+1)^{\varphi}}{\varphi}-\frac{(m+1)^{\varphi+1}}{\varphi+1}\Big)G_m\\ &-\Big(\frac{(m+1)^{\varphi}}{\varphi}-\frac{(m+1)^{\varphi+1}}{\varphi+1}\Big)G_{m-1}\Big].\end{aligned}$$

Similarly the [22] fractional integral $\int_0^{r_m}(t_m-\rho)^{\varphi-1}G(v,\rho)d\rho$ in equation (4.3.3) can be computed as

$$\int_0^{r_m}(r_m-\rho)^{\varphi-1}G(v,\rho)d\rho=\sum_{i=0}^{m-1}\int_{r_i}^{r_{i+1}}(r_m-r)^{\varphi-1}\bigg(\frac{r-r_{m-1}}{r_m-r_{m-1}}G_m+\frac{r-r_m}{r_{m-1}-r_m}G_{m-1}\bigg)dr$$

$$\int_0^{r_m}(r_m-\rho)^{\varphi-1}G(v,\rho)d\rho=\frac{G_m}{k}\sum_{i=0}^{m-1}\int_{r_i}^{r_{i+1}}(r_m-r)^{\varphi-1}(r-r_{m-1})dr-\frac{G_{m-1}}{k}\sum_{i=0}^{m-1}\int_{r_i}^{r_{i+1}}(r_m-r)^{\varphi-1}(r-r_m)dr$$

And changing the [22] variables, we let $z=r_m-r, dr=-dz, r=r_m-z$.

$$\begin{aligned}
\int_0^{r_m}(r_m-\rho)^{\varphi-1}G(v,\rho)d\rho=&\frac{G_m}{k}\sum_{i=0}^{m-1}\int_{r_m-r_i}^{r_m-r_{i+1}}-(z)^{\varphi-1}(r_m-r_{m-1}-z)dz-\frac{G_{m-1}}{k}\sum_{i=0}^{m-1}\int_{r_m-r_i}^{r_m-r_{i+1}}z^{\varphi}dz\\
\int_0^{r_m}(r_m-\rho)^{\varphi-1}G(v,\rho)d\rho=&\frac{G_m}{k}\sum_{i=0}^{m-1}\int_{r_m-r_i}^{r_m-r_{i+1}}(z^{\varphi}-kz^{\varphi-1})dz-\frac{G_{m-1}}{k}\sum_{i=0}^{m-1}\int_{r_m-r_i}^{r_m-r_{i+1}}z^{\varphi}dz\\
\int_0^{r_m}(r_m-\rho)^{\varphi-1}G(v,\rho)d\rho=&\frac{G_m}{k}\sum_{i=0}^{m-1}\bigg[\frac{z^{\varphi+1}}{\varphi+1}-\frac{k}{\varphi}z^{\varphi}\bigg]_{r_m-r_i}^{r_m-r_{i+1}}-\frac{G_{m-1}}{k}\sum_{i=0}^{n-1}\bigg[\frac{z^{\varphi+1}}{\varphi+1}\bigg]_{r_m-r_i}^{r_m-r_{i+1}}\\
=&\frac{G_m}{k}\sum_{i=0}^{m-1}\bigg(\frac{(r_m-r_{i+1})^{\varphi+1}}{\varphi+1}-\frac{k}{\varphi}(r_m-r_{i+1})^{\varphi}-\frac{(r_m-r_i)^{\varphi+1}}{\varphi+1}+\frac{k}{\varphi}(r_m-r_i)^{\varphi}\bigg)\\
&-\frac{G_{m-1}}{k}\sum_{i=0}^{m-1}\bigg(\frac{(r_m-r_{i+1})^{\varphi+1}}{\varphi+1}-\frac{(r_m-r_i)^{\varphi+1}}{\varphi+1}\bigg)\\
=&\frac{G_m}{k}\bigg\{\sum_{i=0}^{m-1}\bigg(\frac{(r_m-r_{i+1})^{\varphi+1}}{\varphi+1}-\frac{(r_m-r_i)^{\varphi+1}}{\varphi+1}\bigg)\\
&-\frac{k}{\varphi}\sum_{i=0}^{m-1}\bigg((r_m-r_{i+1})^{\varphi}-(r_m-r_i)^{\varphi}\bigg)\bigg\}\\
&-\frac{G_{m-1}}{k}\sum_{i=0}^{m-1}\bigg(\frac{(r_m-r_{i+1})^{\varphi+1}}{\varphi+1}-\frac{(r_m-r_i)^{\varphi+1}}{\varphi+1}\bigg)\\
=&\frac{G_m}{k}\bigg\{-\frac{(r_m-r_0)^{\varphi+1}}{\varphi+1}-\frac{k}{\varphi}\bigg(-(r_m-r_0)^{\varphi}\bigg)\bigg\}-\frac{G_{m-1}}{k(\varphi+1)}(-(r_m-r_0)^{\varphi+1})\\
=&\frac{G_m}{k}\bigg(-\frac{(r_m-r_0)^{\varphi+1}}{\varphi+1}+\frac{k}{\varphi}(r_m-r_0)^{\varphi}\bigg)+\frac{G_{m-1}}{k(\varphi+1)}(r_m-r_0)^{\varphi+1}\\
=&\frac{G_m}{k}\bigg(\frac{-m^{\varphi+1}k^{\varphi+1}}{\varphi+1}+\frac{m^{\varphi}k^{\varphi+1}}{\varphi}\bigg)+\frac{m^{\varphi+1}k^{\varphi+1}}{k(\varphi+1)}G_{m-1}
\end{aligned}$$

This, therefore can be written as

$$\int_0^{r_m}(r_m-\rho)^{\varphi-1}G(v,\rho)d\rho=k^{\varphi}\bigg((\frac{m^{\varphi}}{\varphi}-\frac{m^{\varphi+1}}{\varphi+1})G_m+\frac{m^{\varphi+1}}{\varphi+1}G_{m-1}\bigg)$$

Equation (4.3.3) is then rewritten and [22]substituted in the later results which gives

$$\begin{aligned} v_{m+1}-v_m &= \frac{k^{\varphi}}{\Gamma(\varphi)}\left[\left(\frac{2(m+1)^{\varphi}}{\varphi}-\frac{(\varphi+1)^{\varphi+1}}{\varphi+1}\right)G_m\right. \\ &\left.-\left(\frac{(m+1)^{\varphi}}{\varphi}-\frac{(m+1)^{\varphi+1}}{\varphi+1}\right)G_{m-1}-\left(\left(\frac{m^{\varphi}}{\varphi}-\frac{m^{\varphi+1}}{\varphi+1}\right)G_m+\frac{m^{\varphi+1}}{\varphi+1}G_{m-1}\right)\right] \\ v_{m+1}-v_m &= \frac{k^{\varphi}}{\Gamma(\varphi)}\left[\left(\frac{2(m+1)^{\varphi}-m^{\varphi}}{\varphi}+\frac{m^{\varphi+1}-(\varphi+1)^{\varphi+1}}{\varphi+1}\right)G_m\right. \\ &\left.-\left(\frac{(m+1)^{\varphi}}{\varphi}+\frac{m^{\varphi+1}-(m+1)^{\varphi+1}}{\varphi+1}\right)G_{m-1}\right] \end{aligned} \tag{4.3.4}$$

Remark 4.3.1. *[22] Setting $\varphi = 1$ ensures that the classic Adams-Bashforth Numerical scheme is retained.*

$$\begin{aligned} v_{m+1}-v_m =& \frac{k}{\Gamma(1)}(2m+2-m+\frac{m^2-(m+1)^2}{2})G_m-(m+1+m^2-(m+1)^2)G_{m-1} \\ v_{m+1}-v_m =& k(m+2+\frac{1}{2}m^2-\frac{1}{2}m^2-m-\frac{1}{2})G_m-(m+1+m^2-m^2-m-\frac{1}{2})G_{m-1} \\ u_{m+1}-u_m =& k(\frac{3}{2}G_m-\frac{1}{2}G_{m-1}) \end{aligned}$$

We need to return [22] the numerical scheme back in the real space. We achieve this by applying the inverse form of Laplace equation (4.3.4). This gives the algorithm or a numerical scheme that iterates in the real space:

$$\begin{aligned} v_{m+1(u,r)} = \mathscr{L}^{-1}\left\{v_m+\frac{k^{\varphi}}{\Gamma(\varphi)}\left[\left(\frac{2(m+1)^{\varphi}-m^{\varphi}}{\varphi}+\frac{m^{\varphi+1}-(m+1)^{\varphi+1}}{\varphi+1}\right)G_m\right.\right. \\ \left.\left.-\left(\frac{(m+1)^{\varphi}}{\varphi}+\frac{m^{\varphi+1}-(m+1)^{\varphi+1}}{\varphi+1}\right)G_{m-1}\right]\right\} \end{aligned} \tag{4.3.5}$$

4.3.1 The discussion on the Error Analysis of the Method

Consider [22] the general fractional partial differential equation.

$$ {}_0^C D^{\varphi} v(u,r) = Mv(u,r)+Uv(u,r) \tag{4.3.6}$$

As mentioned earlier, the solutions which are numeric that uses the Laplace Adams-Bashforth method, are represented in the following equation as

$$v_{m+1(u,r)} = \mathscr{L}^{-1}\Bigg\{v_m + \frac{k^\varphi}{\Gamma(\varphi)}\Bigg[\Bigg(\frac{2(m+1)^\varphi - m^\varphi}{\varphi} + \frac{m^{\varphi+1} - (m+1)^{\varphi+1}}{\varphi+1}\Bigg)G_m \\ -\Bigg(\frac{(m+1)^\varphi}{\varphi} + \frac{m^{\varphi+1} - (m+1)^{\varphi+1}}{\varphi+1}\Bigg)G_{m-1}\Bigg] + K_m^\varphi\Bigg\} \tag{4.3.7}$$

Where

$$K_m^\varphi < \infty$$

Proof. [22]

$$v_{m+1} - v_m = \frac{1}{\Gamma(\varphi)}\Bigg[\int_0^{r_{m+1}} (r_{m+1} - \rho)^{\varphi-1} G(v,\rho)d\rho - \int_0^{r_m} (r_m - \rho)^{\varphi-1} G(v,\rho)d\rho\Bigg]$$

Where

$$G(v,\xi) = \frac{r - r_{m-1}}{r_m - r_{m-1}}G_m + \frac{r - r_m}{r_{m-1} - r_m}G_{m-1} + \frac{G^{(2)}(v,\xi)}{2!}\prod_{j=0}^{1}(r - r_j)$$

$$v_{m+1} - v_m = \frac{1}{\Gamma(\varphi)}\int_0^{r_{m+1}} (r_{m+1} - r)^{\varphi-1}\Bigg(\frac{r - r_{m-1}}{r_m - r_{m-1}}G_m + \frac{r - r_m}{r_{m-1} - r_m}G_{m-1}\Bigg)dr \\ -\frac{1}{\Gamma(\varphi)}\int_0^{r_m} (r_m - r)^{\varphi-1}\Bigg(\frac{r - r_{m-1}}{r_m - r_{m-1}}G_m + \frac{r - r_m}{r_{m-1} - r_m}G_{m-1}\Bigg)dr \\ +\frac{1}{\Gamma(\varphi)}\int_0^{r_{m+1}} \frac{G^{(2)}(u,\xi)}{2!}\prod_{j=0}^{1}(r - r_j)(r_{m+1} - r)^{\varphi-1}dr \\ -\frac{1}{\Gamma(\varphi)}\int_0^{r_m} \frac{G^{(2)}(v,\xi)}{2!}\prod_{j=0}^{1}(r - r_j)(r_m - r)^{\varphi-1}dr$$

Which gives

$$v_{m+1} - v_m = \frac{k^\varphi}{\Gamma(\varphi)}\Bigg[\Bigg(\frac{2(m+1)^\varphi - m^\varphi}{\varphi} + \frac{m^{\varphi+1} - (m+1)^{\varphi+1}}{\varphi+1}\Bigg)G_m \\ -\Bigg(\frac{(m+1)^\varphi}{\varphi} + \frac{m^{\varphi+1} - (m+1)^{\varphi+1}}{\varphi+1}\Bigg)G_{m-1}\Bigg] + K_m^\varphi$$

We therefore can deduce that

$$K_m^{\varphi} = \frac{1}{\Gamma(\varphi)}\Bigg(\int_0^{r_{m+1}} \frac{G^{(2)}(v,\xi)}{2!}\prod_{j=0}^{1}(r-r_j)(r_{m+1}-r)^{\varphi-1}dr - \int_0^{r_m} \frac{G^{(2)}(v,\xi)}{2!}\prod_{j=0}^{1}(r-r_j)(r_m-r)^{\varphi-1}dr\Bigg)$$

$$|K_m^{\varphi}| \leq \frac{1}{\Gamma(\varphi)}\Bigg(\int_0^{r_{m+1}} \left|\frac{G^{(2)}(v,\xi)}{2!}\prod_{j=0}^{1}(r-r_j)(r_{m+1}-r)^{\varphi-1}\right|dr + \int_0^{r_m} \left|\frac{G^{(2)}(v,\xi)}{2!}\prod_{j=0}^{1}(r-r_j)(r_m-r)^{\varphi-1}dr\right|\Bigg)$$

$$|K_m^{\varphi}| \leq \frac{k^2}{8\Gamma(\varphi)}\underset{\xi\in(0,r_{m+1})}{max}\{G^{(-2)}(v,\xi)\}\Bigg(\int_0^{r_{m+1}} |(r_{m+1}-r)^{\varphi-1}|dr + \int_0^{r_m} |(r_m-r)^{\varphi-1}dr|\Bigg)$$

$$|K_m^{\varphi}| \leq \frac{k^2}{8\Gamma(\varphi)}\underset{\xi\in(0,r_{m+1})}{max}\{G^{(-2)}(v,\xi)\}\left(\frac{r_{m+1}^{\varphi}+r_m^{\varphi}}{\varphi}\right)$$

$$|K_m^{\varphi}| \leq \frac{k^2k^{\varphi}}{8\Gamma(\varphi+1)}\underset{\xi\in(0,r_{m+1})}{max}\{G^{(-2)}(v,\xi)\}(m+1^{\varphi}+m^{\varphi}) < +\infty$$

■

Chapter 5

Application of the method to Partial Differential Equations

We present in this chapter the numerical simulations of the new two-step Laplace Adams-Bashforth method applied to the four-dimensional chaotic model, Caputo-Lu-Chen model and the partial differential equation (wave equation).

5.1 Four-dimensional Model

We first consider values of ϕ where $\phi = 1.08$ and $\phi = 0.4$ respectively, and observe from the simulation of the system (3.3.2) a pattern of butterfly type attractors depicted in figures (5.1)-(5.3). For each of the case of attractors, we have set the control parameters to $\xi = 12, \Phi = 10, \phi = 2$ with the starting values set at $s = 1, h = 0, m = 0, l = 0$. In each of the figures namely (a),(b),(c) and (d) we observe the projections on each plane and they are x and y, x and z, x and w and lastly y and z planes. We also observe equilibrium points that are represented by the blue dots. The dynamics are in fact chaotic and are confirmed by the analysis presented earlier. We further consider the bifurcation diagram depicted in figure(5.4) for the value $\phi = 1$ representing the integer case and $\phi = 0.7$ that is representing the ABC fractional case, showing that the system (3.3.2) has characteristics of standard period doubling, suggesting an irregular behaviour resulting into chaos. The phase portrait dynamics for the system (3.3.2) as shown in figure (5.5) and figure (5.6), respectively for $\phi = 1$ and $\phi = 0.6$ support the assertion. In figure (5.4) we see how period doubling via the phase portrait result into chaotic dynamics. This is achieved by using the control parameters $\alpha = 12, \beta = 10$. The

value of ψ is set at 19, 18, 16,and 14, 98. We have for $\phi = 1$ and $\phi = 0.8$ simulation for the system (3.3.2) depicted in figure (5.7) and figure (5.8) showing a variety of shapes of strange attractors with fractal depictions. These shapes clearly are observable on the x and y, x and z, x and w and finally y and z planes when the respective control parameters are set to $\xi = 12, \Phi = 10$ and $\psi = 1$.

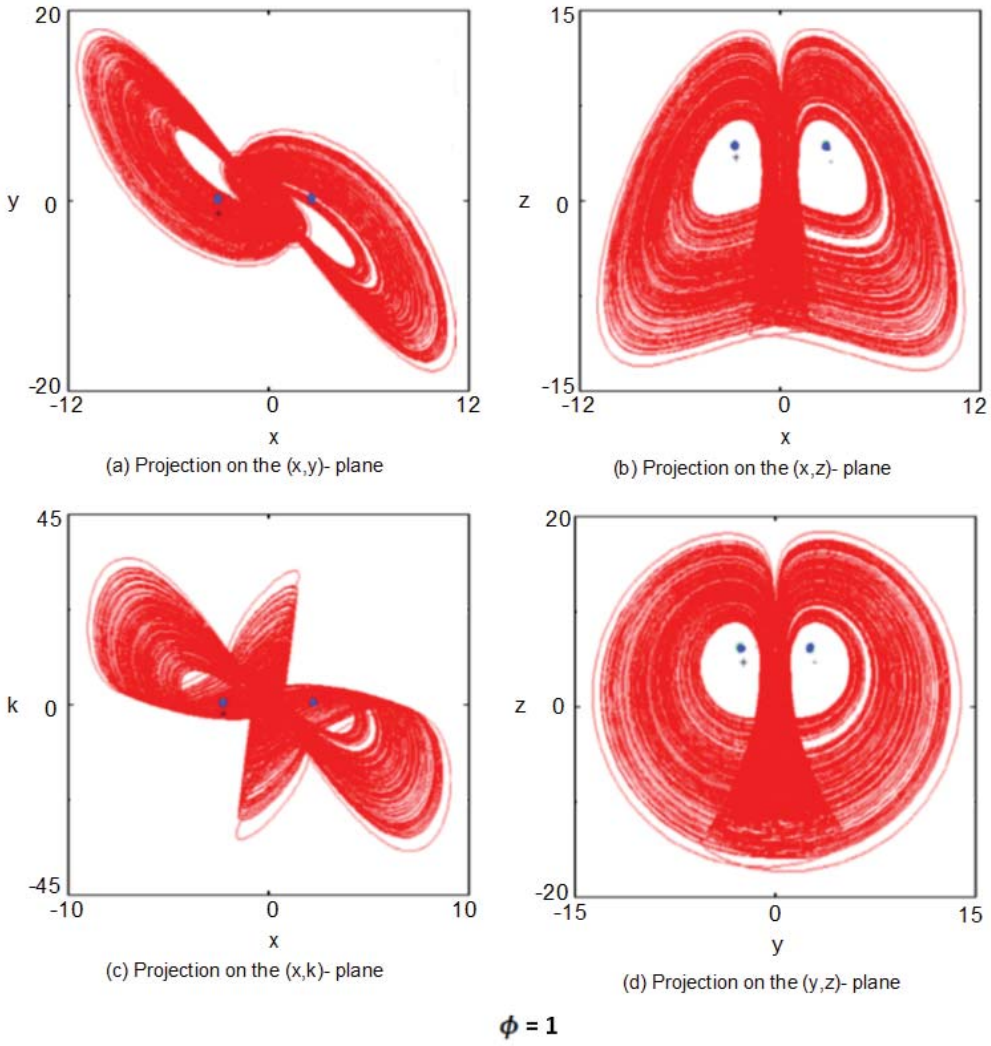

Figure 5.1: The diagram simulates the system (3.3.2) showing the butterfly type attractors for the derivative order set to $\phi = 1$. The control parameters are taken to be $\xi = 12, \Phi = 10, \psi = 2$ for the starting values $s = 1, h = 1, m = 0, l = 0$. These shapes clearly are observable on the x and y, x and z, x and w and finally y and z planes as shown in (a), (b), (c), and (d). Equilibrium points are represented by the blue dots.

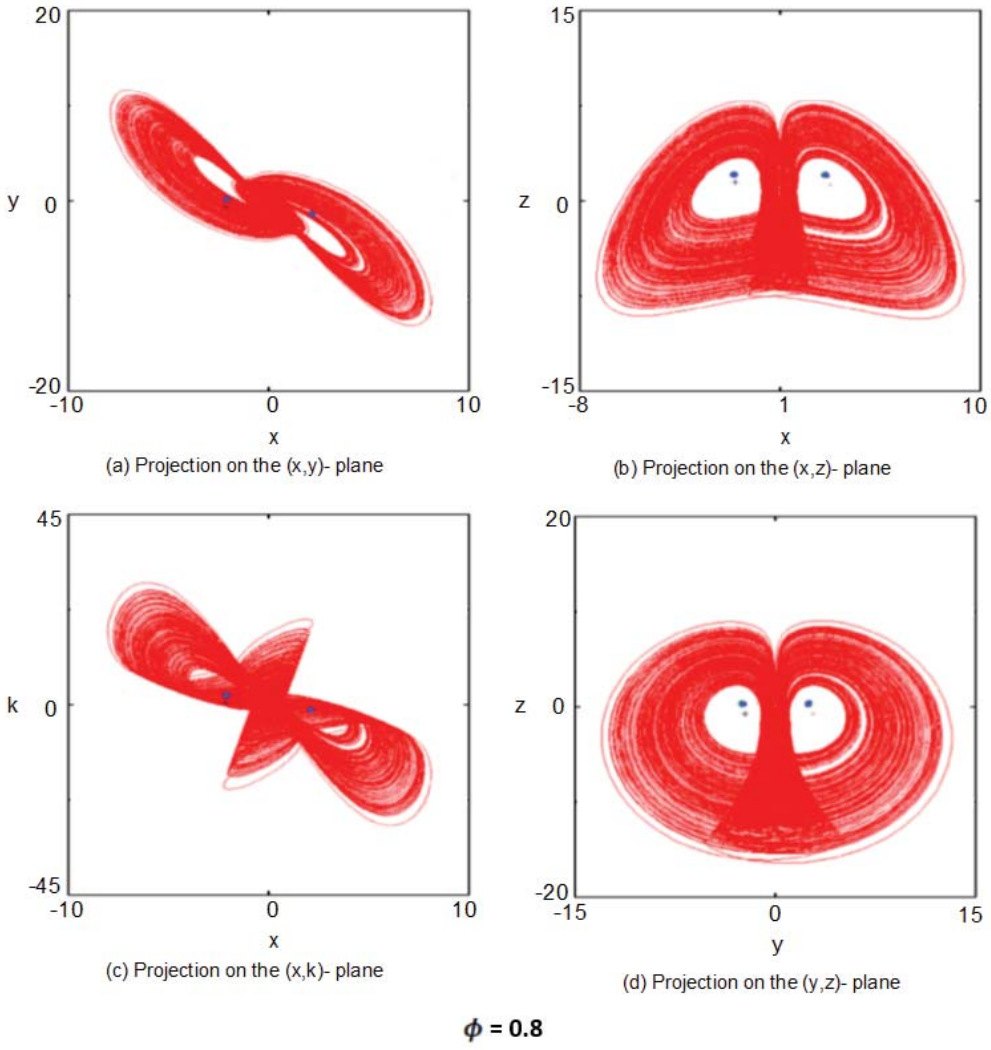

Figure 5.2: The diagram simulates the system (3.3.2) showing butterfly like structure attractors for fractional derivative of order set to $\phi = 0.8$. We set control parameters to be $\xi = 12, \Phi = 10, \psi = 2$ and the starting values are $s = 1, h = 1, m = 0, l = 0$. These shapes clearly are observable on the x and y, x and z, x and w and finally y and z planes. Equilibrium points are shown by the blue dots.

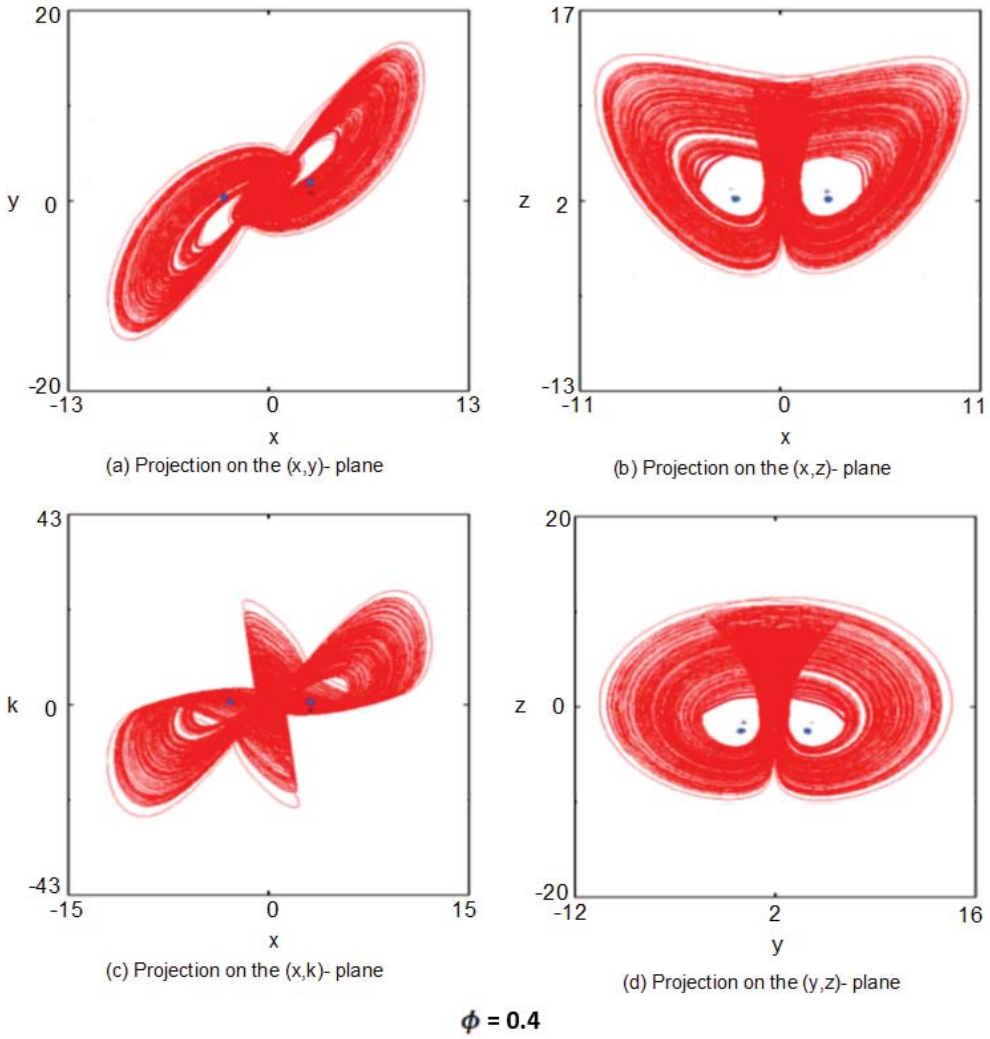

Figure 5.3: The diagram simulates the system (3.3.2) showing butterfly like structure attractors for fractional derivative of order set to $\phi = 0.4$. We set control parameters to be $\xi = 12, \Phi = 10, \psi = 2$ and the starting values are $s = 1, h = 1, m = 0, l = 0$. These shapes clearly are observable on the x and y, x and z, x and w and finally y and z planes respectively, in (a), (b), (c), and (d). Equilibrium points are represented by the blue dots.

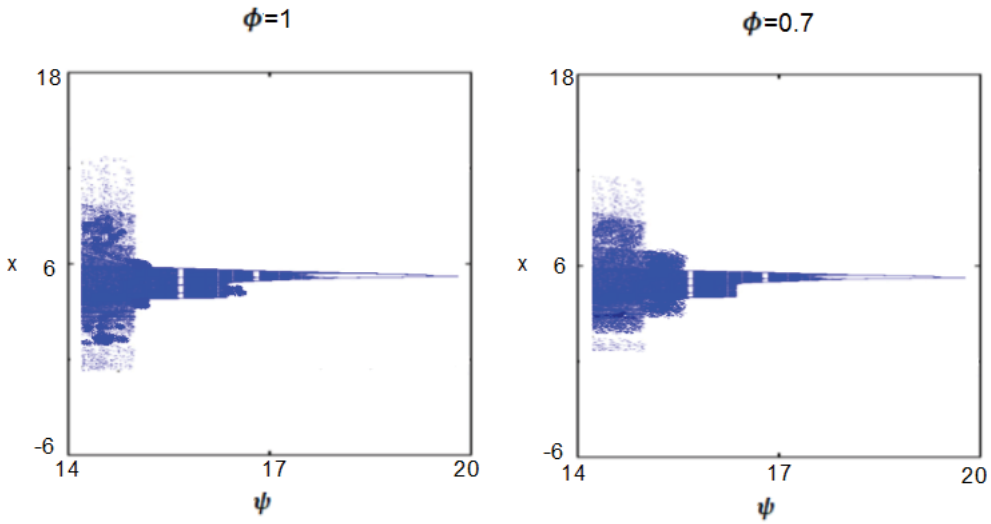

Figure 5.4: The diagram represents the bifurcation of the system (3.3.2) with the control parameters $\alpha = 12, \beta = 10$, and $14 \leq \psi \leq 20$.

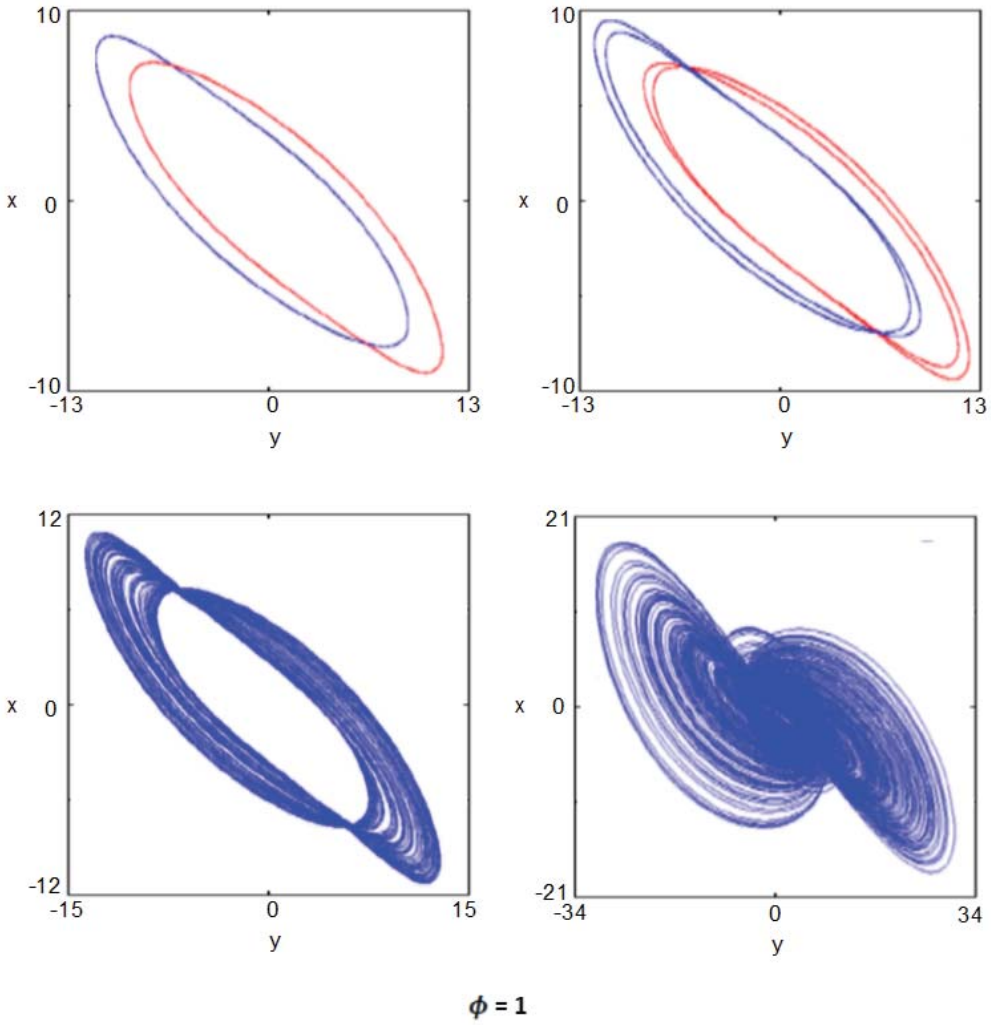

Figure 5.5: The diagram simulates the phase portraits of the system (3.3.2) with $\phi = 1$, clearly depicting how period doubling leading to dynamics that are chaotic in nature. We set control parameters to $\xi = 12, \Phi = 10$, and ψ is set at $19, 18, 16$, and $14, 98,$.

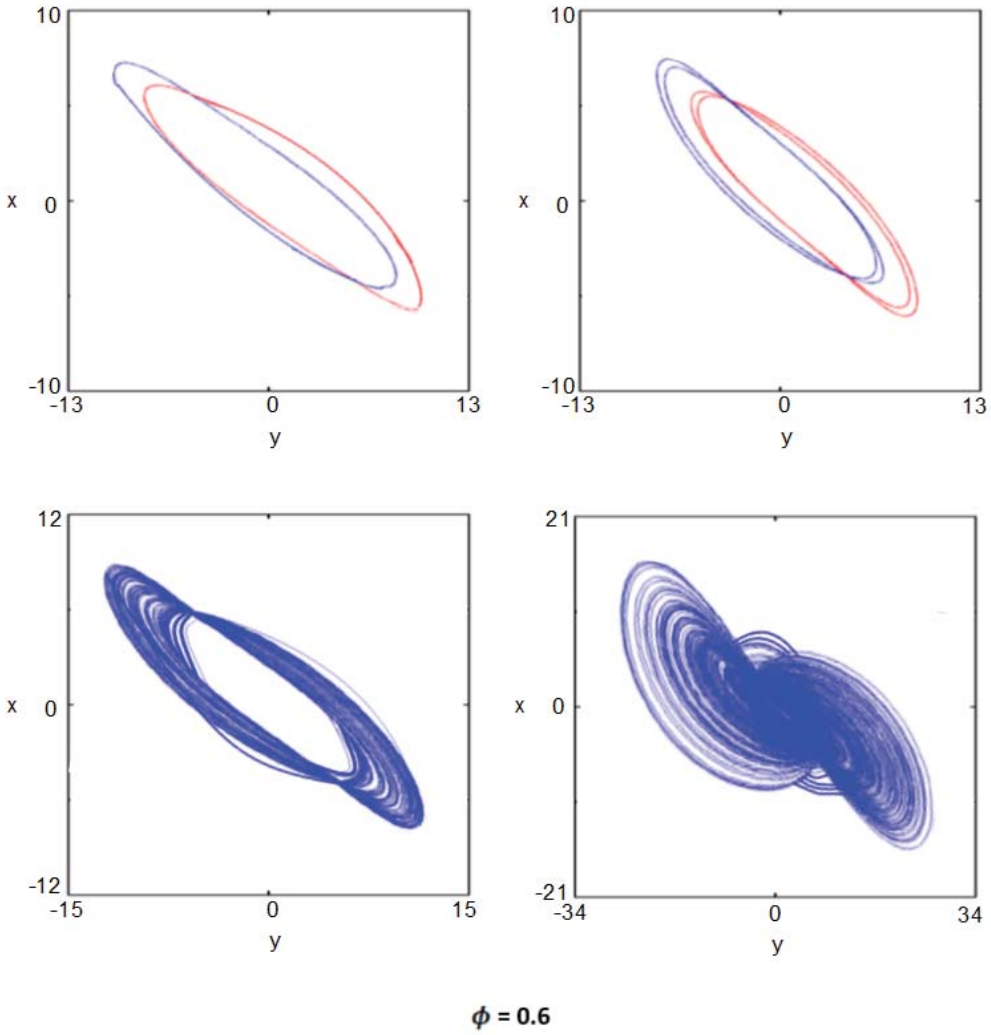

Figure 5.6: The diagram simulates the phase portraits of the system (3.3.2) with $\phi = 0.6$, clearly depicting how period doubling leading to dynamics that are chaotic in nature. We set the control parameters to $\xi = 12, \Phi = 10$, and ψ is set at $19, 18, 16$, and $14, 98,$.

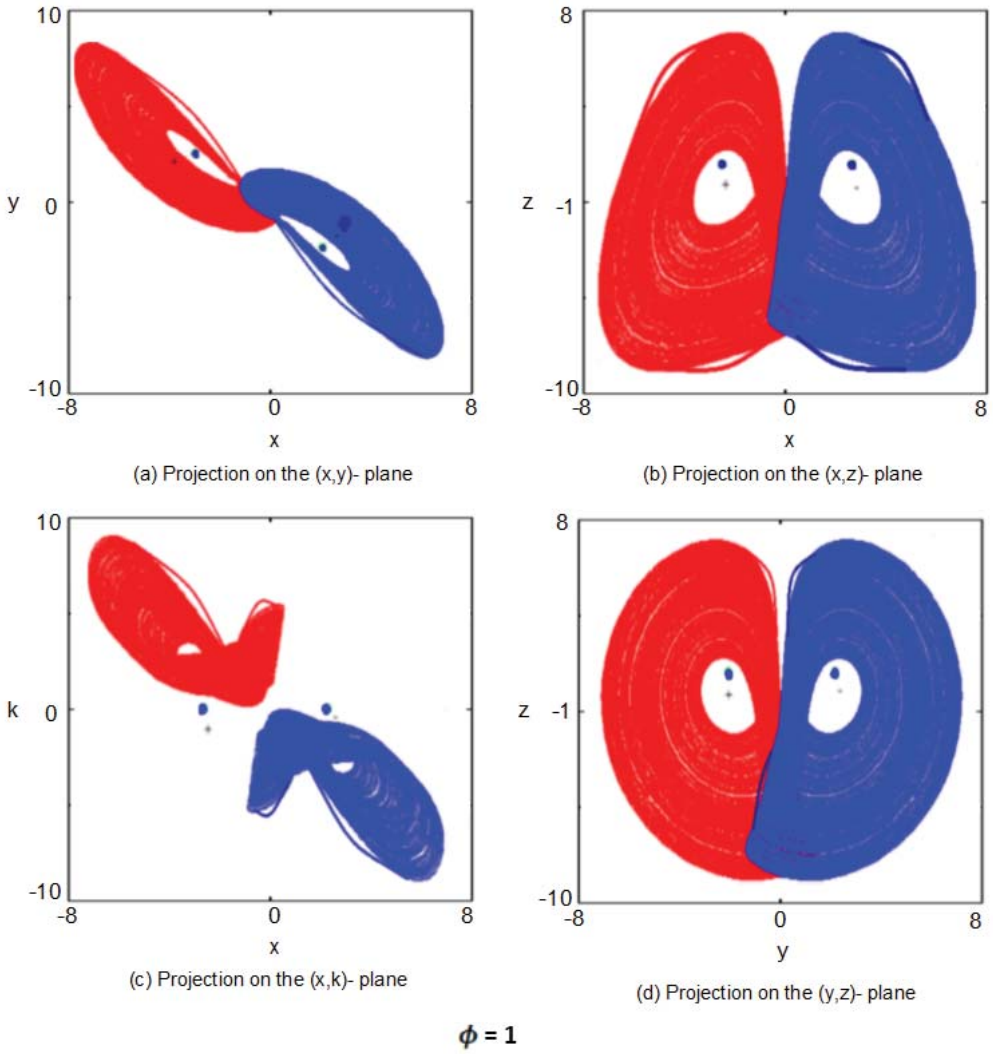

Figure 5.7: The diagram simulates the system (3.3.2) with $\phi = 1$, depicting structures of strange attractors with fractals. The projections on the planes (x,y), (x,z), (x,k), and (y,z) are given by (a), (b), (c), and (d). The equilibrium points are represented by the blue dots. The control parameters are $\alpha = 12, \beta = 10$, and $\psi = 1$.

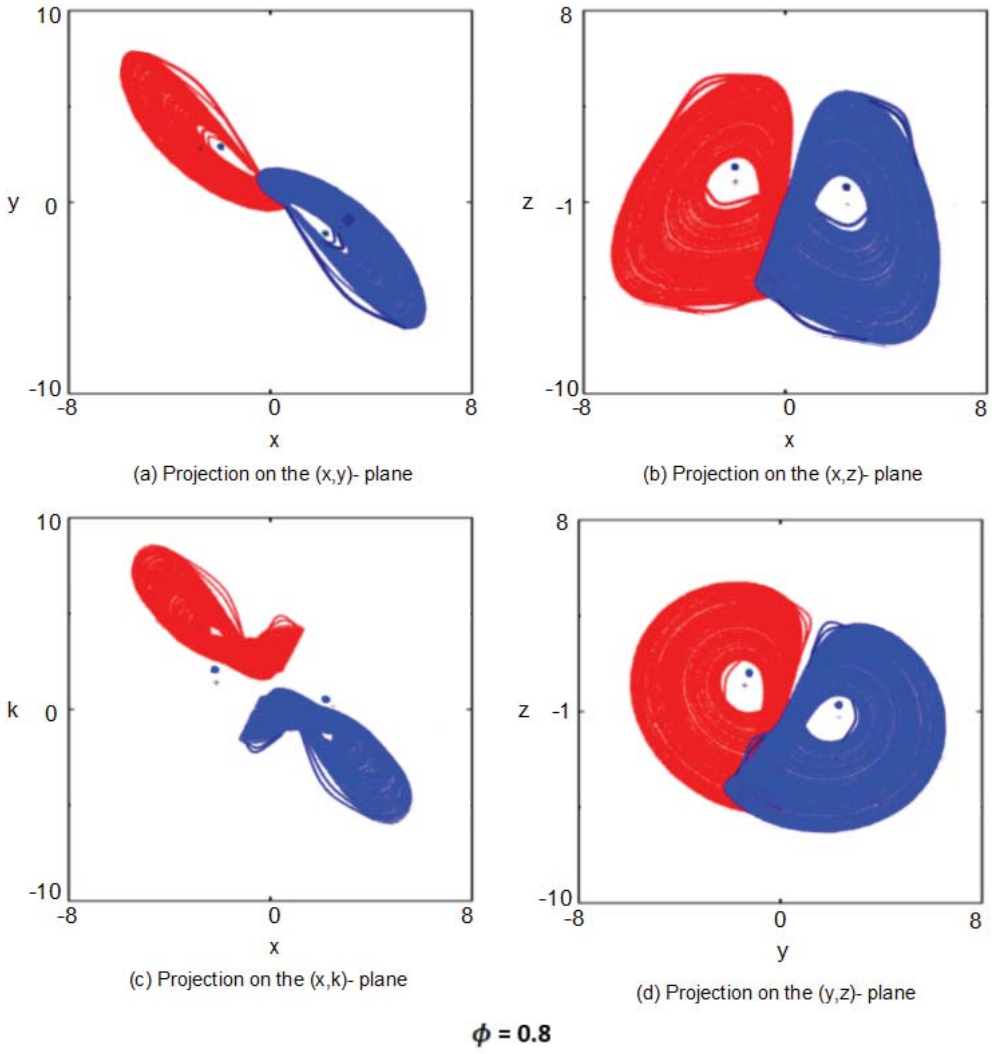

Figure 5.8: The diagram of the numerical simulations for the model (3.3.2) with $\phi = 0.8$. The system shows projections of a pair of strange attractors with a fractal structure. These shapes clearly are observable on the x and y, x and z, x and w and finally y and z planes respectively and are represented in (a), (b), (c), and (d). Equilibrium points are represented by the blue dots. Control parameters are set as $\xi = 12, \Phi = 10$, and $\psi = 1$.

5.2 Caputo-Lu-Chen Model

We look into the Caputo-Lu-Chen model with multiscroll attractor popularly known for its exhibition of chaotic behaviour, mainly when the parameter is assigned some values

and is defined as

$$\begin{aligned} D_t^{\phi}x(t) =&\alpha(y(t)-x(t)),\\ D_t^{\phi}y(t) =&s+x(t[1-z(t)]+ly(t)),\\ D_t^{\phi}z(t) =&x(t)y(t)-\beta z(t), \end{aligned} \tag{5.2.1}$$

where α, β, l, s are parameters of the model for $-15 \leq s \leq 15$. Setting the derivative order $\phi = 1$ gives the Lu-Chen system

$$\begin{aligned} x'(t) =&\alpha(y(t)-x(t)),\\ y'(t) =&s+x(t[1-z(t)]+ly(t)),\\ z'(t) =&x(t)y(t)-\beta z(t), \end{aligned} \tag{5.2.2}$$

with similar variables as in (5.2.1). The generalised model of (5.2.2) is classified to be of strange attractors family as in the (5.2.2) and is given by

$$\begin{aligned} x'(t) =&\alpha(y(t)-g(x)),\\ y'(t) =&x(t)-y(t)+z(t),\\ z'(t) =&-\rho y(t), \end{aligned} \tag{5.2.3}$$

with

$$g(x) = v_{2i-1}x + \frac{1}{2}\sum_{p=1}^{2i-1}(v_{p-1}-v_p)(|x+l_p|-|x-l_pk|$$

and $i \in \mathbb{N}$. The 2D PWL model is an example of a system that is (5.2.2) classified with the chaotic strange attractor group and is given by

$$\begin{aligned} x'(t) =&y(t),\\ y'(t) =&-v_1x(t)-\left(\frac{1}{2(v_0-v_1)}\right)\times(|x(t)+1|-|x(t)-1|-ay(t)+\eta\cos(\theta t), \end{aligned} \tag{5.2.4}$$

with v_p, a, η, θ as variables of the system.

The Lu-Chen model (5.2.2) with $\alpha = 34, \beta = 2, l = 20, s = -12, s = 1$ and $s = 12$ is shown in figures 5.9(a)-5.9(c). We apply the initial conditions set to $x(0) = 1, y(0) = 1, z(0) = 12$ and the model shows characteristics of a chaotic attractors with multiscroll when the variable s varies. The model (5.2.3) with $\alpha = 9, \rho = 14, v_0 = -1/7, v_1 = 2/7, v_2 = -4/7, v_3 = 2/7, v_4 = -4/7, v_5 = 2/7$ and $l_1 = 1, l_2 = 2.1, l_3 = 3.4, l_4 = 8.1, l_5 = 12$ is depicted in figure 5.10(b), and it demonstrates a 3-double-scroll chaotic attractor. In addition, in figure 5.10(b), setting parameters to $\alpha = 9, \rho = 14, v_0 = 0.9/7, v_1 = -3/7, v_2 = -4/7, v_3 = -2.3/7, v_4 = 2.55/7, v_5 = -1.6/7, v_6 = 2.51/7, v_7 = -1.6/7$ and

$l_1 = 1, l_2 = 2.1, l_3 = 3.4, l_4 = 6.1, l_5 = 9, l_6 = 13, l_7 = 24$ demonstrates chaotic attractor with seven double scroll, resembling the Lu-Chua model with multiscroll nature. Finally, we show the 2D PWL Duffing (5.2.4) graphs where $a = 0.22, \eta = 0.14 + 0.05p, v_0 = -0.841a - 1, v_1 = 0.60, \rho = 1, p = -10, p = 1$ and $p = 5$ represented in figures 5.9(a)-5.9(c) we set starting values to $x(0) = 0, y(0) = 0$. These graphs in 5.9(a)-5.9(c) clearly demonstrates chaotic attractor of multiscroll nature for the varying variable p.

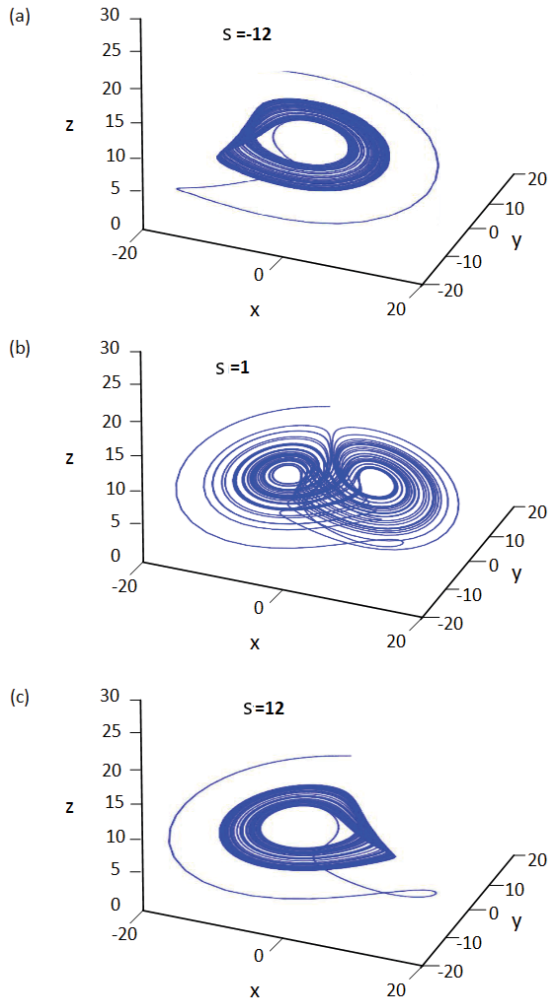

Figure 5.9: Lu–Chen model (5.2.2) depicting chaotic dynamic with initial condition set to $x(0) = 1, y(0) = 1, z(0) = 12$ and with control variables set to $\alpha = 34, \beta = 2, l = 20, s = -12, s = 1$ and $s = 12$. As the variable s changes, the resulting chaos is the attractor of multi wings.

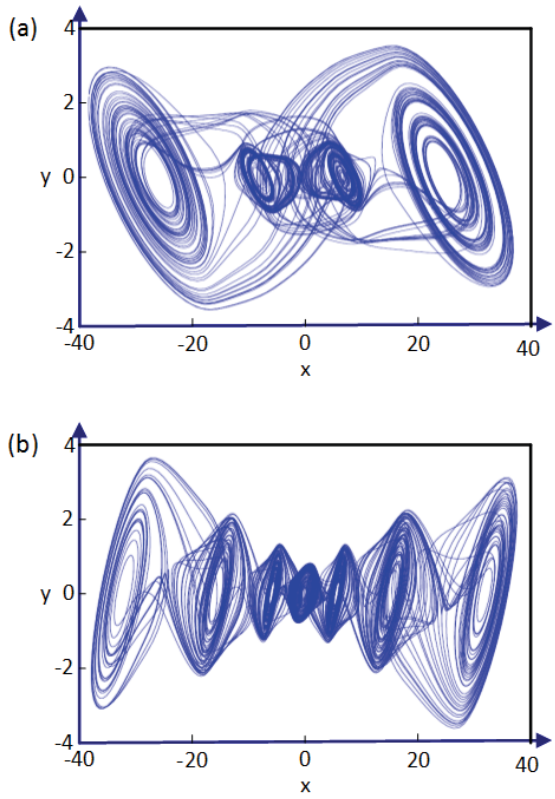

Figure 5.10: Lu–Chen model (5.2.3) depicting chaotic dynamic. The multiscroll character is clearly visible in (a) and the control variables are set to $\alpha = 9, \rho = 14, v_0 = -1/7, v_1 = 2/7, v_2 = -4/7, v_3 = 2/7, v_4 = -4/7, v_5 = 2/7$ and $l_1 = 1, l_2 = 2.1, l_3 = 3.4, l_4 = 8.1, l_5 = 12$. We have in (b), chaotic attractor resembling the 7 bi-scroll for the control variables set to $\alpha = 9, \theta = 14, v_0 = 0.9/7, v_1 = -3/7, v_2 = -4/7, v_3 = -2.3/7, v_4 = 2.55/7, v_5 = -1.6/7, v_6 = 2.51/7, v_7 = -1.6/7$ and $l_1 = 1, l_2 = 2.1, l_3 = 3.4, l_4 = 6.1, l_5 = 9, l_6 = 13, l_7 = 24$.

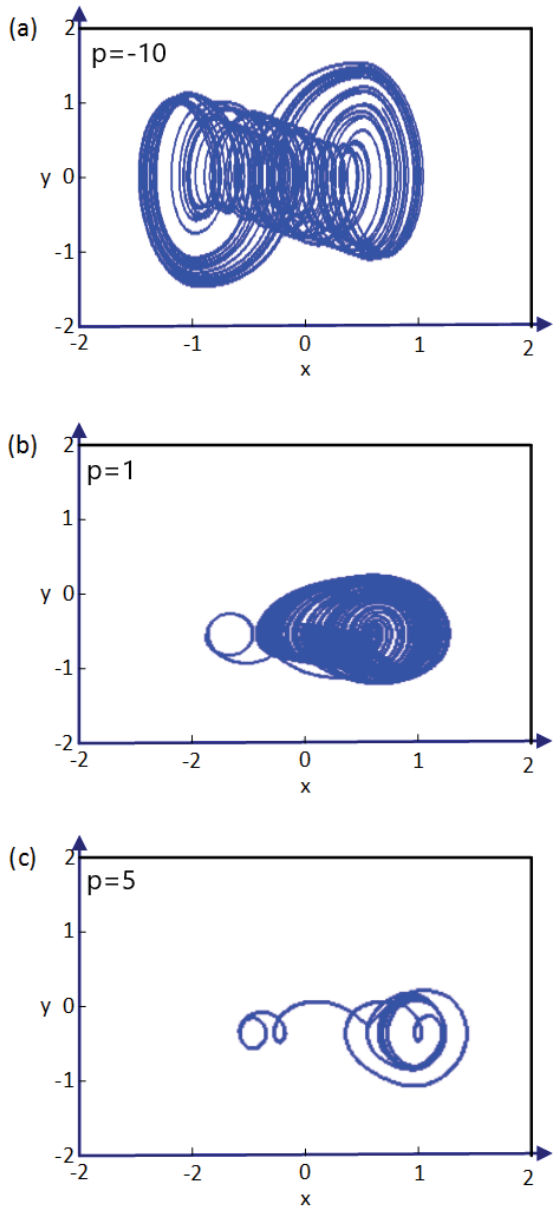

Figure 5.11: The PWL Duffing model (5.2.4) showing the chaotic dynamic. We set the control variables to $a = 0.22, \rho = 0.14 + 0.05p, v_0 = -0.841a - 1, v_1 = 0.60, \theta = 1$. As the variable p varies, the multiscroll chaotic attractors are demonstrated.

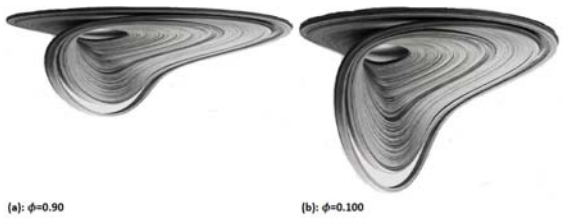

Figure 5.12: The Caputo model (5.2.1) showing the rough chaotic multiwing attractor in its fractional version (a) and in (b) which is the common version. We set the control variables to $\alpha = 35, \beta = 3, l = 18, s = 10$.

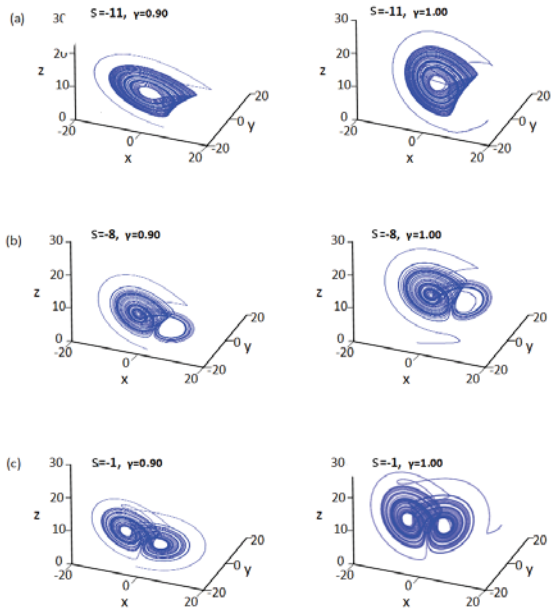

Figure 5.13: Caputo–Lu–Chen model (5.2.1), showing chaotic dynamic. We set the starting values to $x(0) = 1, y(0) = 1, z(0) = 12$. Next, we set control variables to $\alpha = 34, \beta = 2, l = 20$. We further set $s = -11, s = -8$ and $s = -1$. Setting ($\phi = 0.90$) for the fractional derivative and ($\phi = 1.00$) for the normal integer, we observe that the two cases present similar features. Features that are chaotic and manifest themselves as attractors with structure of several scrolls for changing variable s. Observation on the parameter ϕ, shows that the multiscroll property of the attractor is kept unchanged and simply acts as a control parameter while altering the dynamics of the system.

The Caputo-Lu-Chen model (5.2.1) is not only chaotic as depicted in figure (5.12)-(5.14) but also shows features of a multiscroll attractors quite the same as the strange attractors. The multiwing chaotic attractors are seen in figures (5.12)(a) and (5.12)(b) respectively for the fractional case where we set $\phi = 0.9$ and the standard case where we set $\phi = 1$, with control parameters set as: $\alpha = 35, \beta = 3, l = 18, s = 10$. The model with

(5.2.1) begining values set to $x(0) = 1, y(0) = 1, z(0) = 12$ and the control variables set to $\alpha = 34, \beta = 2, l = 20$ for some $s = -11, s = -8$ and $s = -1$ shows chaotic dynamics in figure (5.13) and (5.14). We have for fractional derivative $\phi = 0.90$ and the normal integer $\phi = 1.00$, with the graphs demonstrating features that are similar with chaotic attractor situations of multiple scrolls while the variable s is varied. As the variable ϕ is introduced, Lu-Chen system maintains the characteristics of multi propagated scroll attractors. We also find that the parameter ϕ is regarded as a control variable while altering the dynamic behaviour of the entire model.

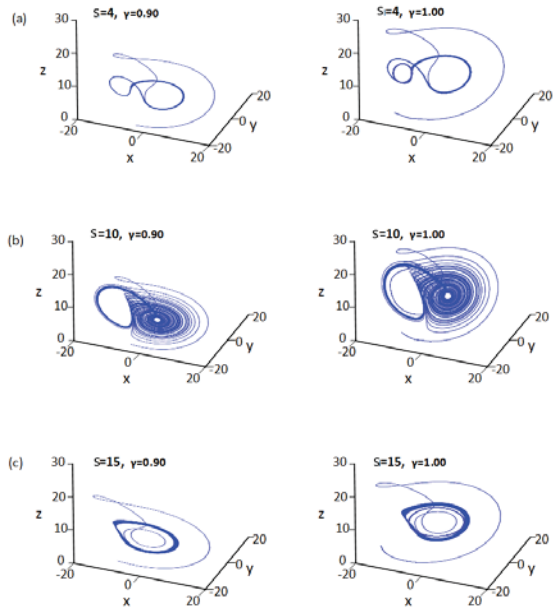

Figure 5.14: The picture shows the Chaotic dynamic of the Caputo–Lu–Chen model (5.2.1), Setting the initial values to $x(0) = 1, y(0) = 1, z(0) = 12$ and setting control variables to $\alpha = 34, \beta = 2, l = 20$. We also set $s = 4, s = 10$ and $s = 15$. Setting $(\phi = 0.90)$ for the fractional derivative case and $(\phi = 1.00)$ for the normal integer case, we observe that the two cases present similar features. Features that are chaotic and manifest themselves as attractors with multi scrolls structure for a changing variable s. Observation on the variable ϕ, shows that the multiscroll property of the attractor is kept unchanged and simply acts as a control parameter while altering the dynamics of the entire system.

5.3 Partial differential equation

Let

$$\frac{\partial U(x,t)}{\partial t} = c\frac{\partial U(x,t)}{\partial x}, \tag{5.3.1}$$

and the discretised wave equation

$$U_j^{n+1} = (1 - \frac{3hc}{2l})U_j^n + \frac{3hc}{2l}U_{j+1}^n - \frac{hc}{2l}U_{j+1}^{n-1} + \frac{hc}{2l}n_j^{n-1}. \tag{5.3.2}$$

The graph represents the numerical simulation of the exact solution of the wave equation (5.3.1) with given value for $c = 3$, initial condition $U(x, 0) = e^x$ and boundary condition $U(0, t) = e^{ct}$ and is depicted in figure 5.15.

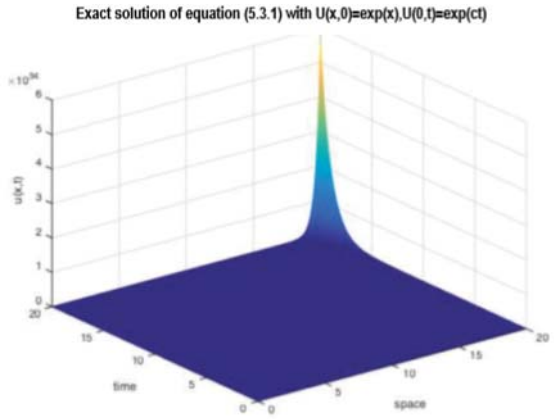

Figure 5.15: The graph of solution of a partial differential equation (5.3.1) with $U(x, 0) = e^x$ and $U(0, t) = e^{ct}$.

The graph in 5.16, depicts a simulation of the approximated solution for the wave partial differential equation (5.3.1) represented in (5.3.2) where $c = 1$, with initial condition $u(x, 0) = e^x$ and boundary condition $u(0, t) = e^t$

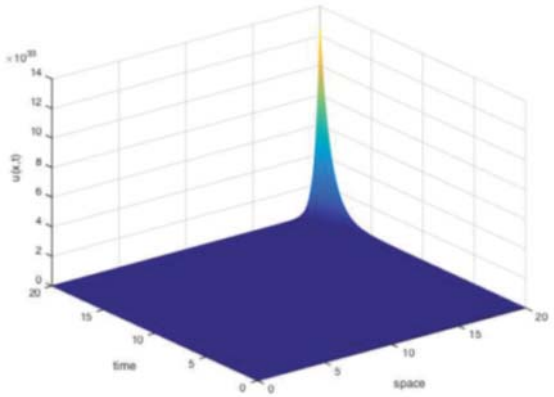

Figure 5.16: The solution of the Approximated partial differential equation (5.3.1) with $U(x, 0) = e^x$ and $U(0, t) = e^{ct}$.

The exact solution of (5.3.1) where $c = 3$, with initial condition $U(x, 0) = \cos x$ and the corresponding boundary condition $U(0, t) = \cos ct$, is shown in figure 5.17

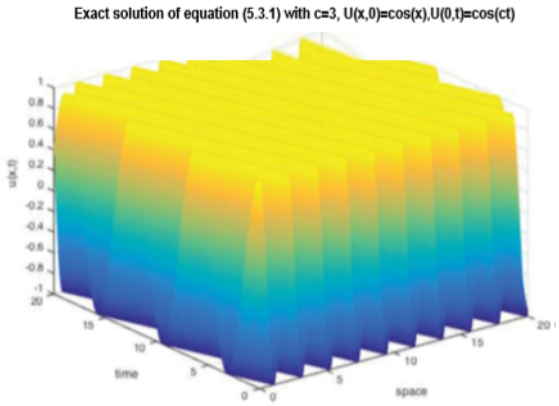

Figure 5.17: Depicted in this grpah is the exact Solution of partial differential equation (5.3.1) for $U(x, 0) = \cos x$ and $U(0, t) = \cos ct$.

Lastly in 5.18, is some numerical simulation of the approximate solution of (5.3.1) given by (5.3.2) where $c = 3, h = 0.001, l = (3*h)/(16*c)$ with initial condition $u(x, 0) = \cos x$ and boundary condition $u(0, t) = \cos ct$

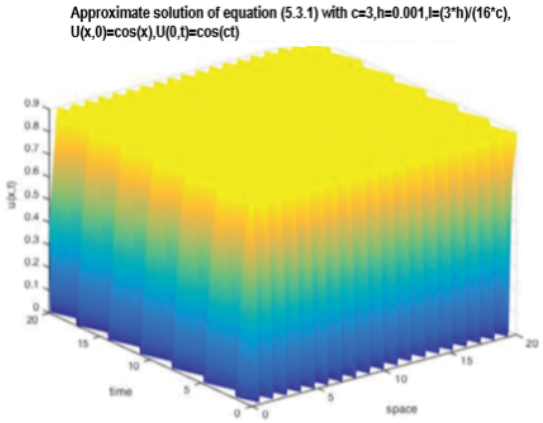

Figure 5.18: The graph depicting the approximation of the partial differential equation (5.3.1) for $U(x, 0) = \cos x$ and $U(0, t) = \cos ct$.

Chapter 6

Conclusion

At the end of this dissertation, it is now clear that the Adams-Bashforth method is fully applicable to real life and natural phenomena. One of its impact is to unveil and display some features of those phenomena that were still hidden until now. Indeed, after we have introduced in the first chapter, the preliminary concepts that form part of the development of the Laplace Adams-Bashforth method, we were able to easily and comfortably analyse the four-dimensional hyperchaotic model. This led to the Laplace Adams-Bashforth numerical scheme to be derived and the error analysis relating to the derived numerical scheme to be presented.

A new method that combines the Adams-Bashforth and Laplace transform was derived by extending the [22] numerical scheme to PDEs with non-integer order derivatives. This is the numerical algorithm that is easy to implement on fractional partial differential equations. The crucial part for the new numerical scheme which is error analysis was discussed and analysed and it was found to converge. This new method was illustrated by applying it on the four-dimensional chaotic system, Caputo-Lu-Chen model and the partial differential equation (wave equation), demonstrating that the new two-step Laplace Adams-Bashforth method is stable and converges. It thus also becomes a useful tool to solve partial differential equations of linear and nonlinear order with non-local and local kernels.

Lastly, the work performed in the course of this dissertation is aligned with the ongoing and current research's trends that was recently developed following great and fierce discussions among authors and researchers regarding the non-validity of the index law in the domain of calculus with fractional differentiation, where non-local operators are used. Useful properties of Mittag-Leffler function that serves here as the kernel have become evident and clearly identifiable. Hence, this dissertation improves the works already accomplished in the domain by revealing other important features of the mathematical

operators with non-local and non-singular kernel in application to dynamical systems that model natural phenomena in the form of chaotic models.

Bibliography

[1] Adem Kilicman Abdon Atangana. A novel integral operator transform and its application to some fode and fpde with some kind of singularities. *Mathematical Problems in Engineering*, 2013:7, 2017.

[2] Aydin Secer Abdon Atangana. The time-fractional coupled-korteweg-de-vries equations. *Abstract and Applied Analysis*, 2013:8, 2013.

[3] Dumitru Baleanu Abdon Atangana. New fractional derivatives with nonlocal and non-singular kernel: Theory and application to heat transfer model. *Thermal Science*, 20, 01 2016.

[4] Emile Franc Doungmo Goufo Abdon Atangana. Conservatory of kaup-kupershmidt equation to the concept of fractional derivative with and without singular kernel. *Acta Mathematicae Applicatae Sinica-English Series*, 34, 2018.

[5] Ilknur Koca Abdon Atangana. Chaos in a simple nonlinear system with atangana–baleanu derivatives with fractional order. *Chaos Solitons and Fractals*, 89:447–454, 2016.

[6] J.M.S. Suarez A.G.O. Goulart, M.J. Lazo and D.M. Moreira. Fractional derivative models for atmospheric dispersion of pollutants. *Physica A*, 2017.

[7] José Francisco Gómez Aguilar and Margarita Miranda Hernández. Space-time fractional diffusion-advection equation with caputo derivative. *Abstract and Applied Analysis*, 2014:8, 2014.

[8] Nakhlé H. Asmar. *Partial Differential Equations with Fourier Series and Boundary Value Problems*. Pearson Hall, second edition, 2005.

[9] Abdon Atangana and Emile Franc Doungmo Goufo. Extension of matched asymptotic method to fractional boundary layers problems. *Mathematical Problems in Engineering*, 2014:7, 2014.

[10] Abdon Atangana and Aydin Secer. A note on fractional order derivatives and table of fractional derivatives of some special functions. *Abstract and Applied Analysis*, 2013:8, 2017.

[11] Wade W.Huebsch Bruce R. Munson, Ted H.Okiishi and Alrie P. Rothmayer. *Fluid Mechanics*. Wiley, seventh edition, 2013.

[12] Lin Cao. A four-dimensional hyperchaotic finance system and its control problems. *Journal of Control Science and Engineering*, 2018:12, 2018.

[13] Joan Dykes and Ronald Smith. *Finite Mathematics with Calculus*. HarperPerenial, first edition, 1993.

[14] A. Kubeka Emile Franc Doungmo Goufo. Approximation result for non-autonomous and non-local rock fracture models. *Japan Journal of Industrial and Applied Mathematics*, 35:217–233, 2018.

[15] JJ Nieto Emile Franc Doungmo Goufo. Attractors for fractional differential problems of transition to turbulent flows. *Journal of Computational and Applied Mathematics*, 339:329–342, 2018.

[16] M. Kamga Pene Emile Franc Doungmo Goufo, R. Maritz. Mathematical & ecological analysis of the effects of petroleum oil droplets braking up and spreading in aquatic environment. *International Journal Of Environment And Pollution*, 61:64–71, 2017.

[17] S. Mugisha Emile Franc Doungmo Goufo. Complex harmonic poles in the evolution of macromolecules depolymerization. *Journal Of Computational Analysis And Applications*, 25:1490–1503, 2018.

[18] Z. Ali Emile Franc Doungmo Goufo, P. Tchepmo and A. Kubeka. A comparative analysis of the harry dym model with and without singular kernel. *Journal Of Computational Analysis And Applications*, 25:228–240, 2018.

[19] Yuan Gao and Chenghua Liang. A new 4d hyperchaotic system and its generalized function projective synchronization. *Mathematical Problems in Engineering*, 2013:13, 2013.

[20] Walter Gautschi. *Numerical Analysis*. Springer, secnd edition, 2012.

[21] Curtis F. Gerald and Patrick O. Wheatley. *Applied Numerical Analysis*. Pearson Addisn Wesley, seventh edition, 2004.

[22] Rodrigue Gnitchogna and Abon Atangana. New Two Step Laplace Adam-Bashfort Method for Integer and Non Integer Order Partial Differential Equations. *Numerical Methods for Partial Differential Equations*, 34:1739–1758, 2017.

[23] Emile Franc Doungmo Goufo. Chaotic processes using the two-parameter derivative with non-singular and non-local kernel: Basic theory and applications. *An interdisciplinary Journal of Nonlinear Science*, 26, 2016.

[24] Emile Franc Doungmo Goufo. Stability and convergence analysis of a variable order replicator-mutator process in a moving medium. *Journal of Theoretical Biology*, 403:178–187, 2016.

[25] Emile Franc Doungmo Goufo. Evolution equations with a parameter and application to transport-convection differential equations. *Turkish Journal Of Mathematics*, 41:636–654, 2017.

[26] Emile Franc Doungmo Goufo. An application of the caputo-fabrizio operator to replicator-mutator dynamics: Bifurcation, chaotic limit cycles and control. *The European Physical Journal Plus*, 133, 2018.

[27] Emile Franc Doungmo Goufo. Mathematical analysis of peculiar behavior by chaotic, fractional and strange multiwing attractors. *International Journal of Bifurcation and Chaos*, 28:14, 2018.

[28] Emile Franc Doungmo Goufo. Strange attractor existence for non-local operators applied to four-dimensional chaotic systems with two equilibrium points. *Chaos*, 2018.

[29] Emile Franc Doungmo Goufo and Abdon Atangana. Analytical and numerical schemes for a derivative with filtering property and no singular kernel with applications to diffusion. *THE EUROPEAN PHYSICAL JOURNAL PLUS*, 131, 2016.

[30] Emile Franc Doungmo Goufo and S. Kumar. Shallow water wave models with and without singular kernel: Existence, uniqueness and similarities. *Mathematical Problems in Engineering*, 2017:9, 2017.

[31] Emile Franc Doungmo Goufo and Ignace Tchangou Toudjeu. Around chaotic disturbance and irregularity for higher order travelling waves. *Journal of Mathematics*, 2018:11, 2018.

[32] Richard Haberman. *Applied Partial Differential Equations with Fourier Series and Boundary Value Problems*. Pearson Education, 5th edition, 2014.

[33] Alexandre Hardy and Willi-Hans Steeb. *Mathematical Tools in Computer Graphics with C sharp Implementation*. World Scientific, 2008.

[34] Dumitru Baleanu H.Jafari, M.Nazari and C.M.Khalique. A new approach for solving a system of fractional partial differential equations. *Comuters and Mathematics with Applications*, 66:838–843, 2013.

[35] Rabha W. Ibrahim and Hamid A. Jalab. The fractional complex step method. *Discrete Dynamics in Nature and Society*, 2013:8, 2013.

[36] Nuo Jia and Tao Wang. Generation and modified projective synchronization for a class of new hyperchaotic systems. *Abstract and Applied Analysis*, 2013:11, 2013.

[37] Lifeng Ma Jiqin Deng. Existence and uniqueness of solutions of initial value problems for nonlinear fractional differential equations. *Applied Mathematics Letters*, 23:676–680, 2010.

[38] Ilknur Koca and Abdon Atangana. *Existence and Uniqueness Results for a Novel Complex Chaotic Fractional Order System*, pages 97–115. Springer International Publishing, Cham, 2019.

[39] Ilknur Koca and Abdon Atangana. *Modulating Chaotic Oscillations in Autocatalytic Reaction Networks Using Atangana?Baleanu Operator*, pages 135–158. Springer International Publishing, Cham, 2019.

[40] Mihailo Lazarević, Milan Rapaić, and Tomislav Šekara. *Introduction to Fractional Calculus with Brief Historical Background*, pages 3–16. 01 2014.

[41] Randall J. LeVeque. *Finite Difference Methods for Ordinary and Partial Differential Equations Steady-Sate and Time-Dependent Problems*. Society for Industrial and Applied Mathematics, 2007.

[42] Peng Jigen Li Kexue. Laplace transform and fractional differential equations. *Applied Mathematics Letters*, 24:2019–2023, 2011.

[43] Ehab Malkawi. Spatial rotation of the fractional derivative in two-dimensional space. *Advances in Mathematical Physics*, 2015:8, 2015.

[44] MojtabaRanjbar Mohammad AliMohebbi Ghandehari. A numerical method for solving a fractional partial differential equation through converting it into an nlp problem. *Comuters and Mathematics with Applications*, 65:975–982, 2013.

[45] Zaid M. Odibat. Analytic study on linear systems of fractional differential equations. *Computers and Mathematics with Applications*, 59:1171–1183, 2010.

[46] Shouquan Pang and Yongjian Liu. A new hyperchaotic system from the Lü system and its control. *Journal of Computational and Applied Mathematics*, 235:2775–2789, 2011.

[47] K S Govinder PM Tchepmo Djomegni and Emile Franc Doungmo Goufo. Movement, competition and pattern formation in a two prey–one predator food chain model. *Computational and Applied Mathematics*, 37:2554–2459, 2018.

[48] Douglas J. Faires Richard L. Burden and Annette M. Burden. *Numerical Analysis*. Cengage Learning, 10 edition, 2016.

[49] Goerge B. Thomas Jr Ross L. Finney. *Calculus*. Addison Wesley, second edition, 1994.

[50] Maurice D. Weir Ross L. Finney and Frank R. Giordano. *Thomas' Calculus*. Addison Wesley, Updated Tenth edition, 2003.

[51] P. G. Dlamini S. S. Motsa and M. Khumalo. Solving hyperchaotic systems using the spectral relaxation method. *Abstract and Applied Analysis*, 2012:18, 2012.

[52] Cao Hui Si Gang-Quan and Zhang Yan-Bin. A new four-dimensional hyperchaotic lorenz system and its adaptive control. *Chin.Phys.B*, 20:1, 2011.

[53] Ercília Sousa. Fractional calculus : Integral and differential equations of fractional order. *International Centre for Mechanical Sciences*, 54:223–276, 2000.

[54] Ercília Sousa. Numerical approximations for fractional diffusion equations via splines. *Computers and Mathematics with Applications*, 62:938–944, 2011.

[55] Willie-Hans Steeb. *The Nonlinear Workbook*. World Scientific, 6th edition, 2015.

[56] Rubayyi T. Alqahtani. Atangana-baleanu derivative with fractional order applied to the model of groundwater within an unconfined aquifer. *Journal of Nonlinear Sciences and Applications*, 9:3647–3654, 06 2016.

[57] Bo Wang and Xiucheng Dong. Secure communication based on a hyperchaotic system with disturbances. *Mathematical Problems in Engineering*, 2015:7, 2015.

[58] Yorick Hardy Willi-Hans Steeb. *Problems and Solutions in Introductory and Advanced Matrix Calculus*. World Scientific, second edition, 2016.

[59] Baojie Zhang and Hongxing Li. A new four-dimensional autonomous hyperchaotic system and the synchronization of different chaotic systems by using fast terminal sliding mode control. *Mathematical Problems in Engineering*, 2013:8, 2013.

[60] Dennis G. Zill and Michael R. Cullen. *Differential Equations with Boundary-Value Problems*. Brooks/Cole Cengage Learning, seventh edition, 2011.

Index